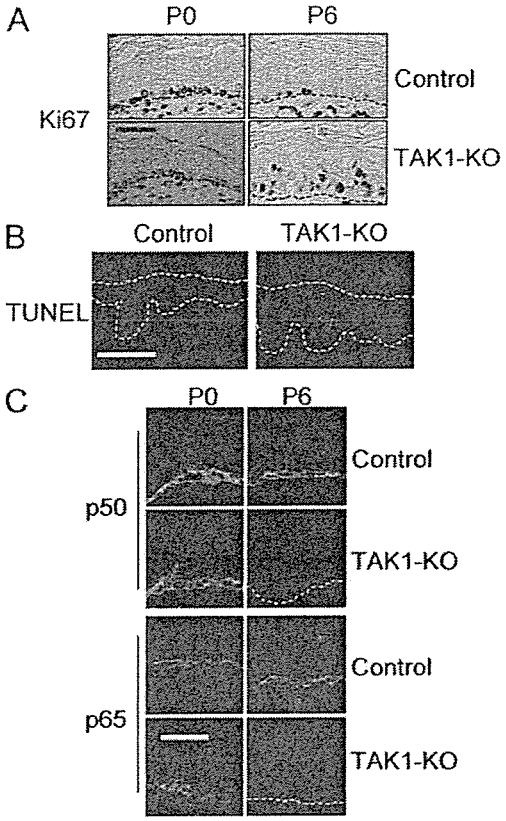

FIGURE 5. **Immunohistochemical analysis of the epidermis of TAK1-KO mice.** *A*, increased proliferation of keratinocytes in the epidermis of TAK1-KO mice. Paraffin-embedded skin sections from TAK1-KO mice at P0 and P6 were stained immunohistochemically with anti-Ki67 antibody. The *dotted lines* indicate the basement membrane. *Scale bar*, 10 μm. *B*, increased apoptosis in the epidermis of TAK1-KO mice. Keratinocyte apoptosis was detected in paraffin-embedded skin sections of TAK1-KO mice at P6 by using the TUNEL method. The signal was observed under a fluorescence microscope. The *dotted lines* indicate the basement membrane and the surface of the epidermis. *Scale bar*, 20 μm. *C*, decreased expression of p50 and p65 in the epidermis of TAK1-KO mice. Frozen skin sections from TAK-KO mice at P0 and P6 were stained with anti-p50 and anti-p65 antibodies. The primary antibody was detected with Alexa Fluor 488-labeled second antibody. Fluorescence was observed under a confocal laser scanning microscope. *Scale bar*, 10 μm.

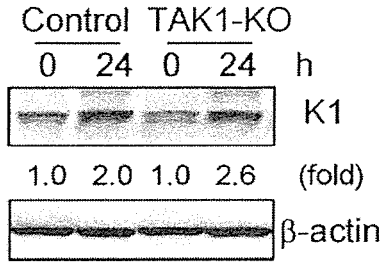

FIGURE 6. **Induction of K1 in TAK1-KO mouse keratinocytes in suspension culture.** Freshly isolated keratinocytes were seeded on culture plates and incubated overnight. To induce differentiation, the adherent cells were subjected to suspension culture using poly-HEMA-coated plates. Western blot analysis was performed to analyze the expression of K1. β-Actin is an internal standard. The intensity of each band was quantified relative to the control, set at one unit.

No microbial pathogens were seen in the micro-abscesses on staining the specimens with methylene blue (data not shown), indicating that the micro-abscesses were not caused by infection. Because the micro-abscesses were associated with keratinocyte apoptosis, one possible mechanism for micro-abscess formation is the release of cytokines or chemokines from dead keratinocytes.

Abnormal Differentiation and Increased Proliferation of Keratinocytes in TAK1-KO Mice—To analyze the differentiation status of epidermal keratinocytes, we performed immunohistochemical analysis of the skin using antibodies against differentiation markers (Fig. 4). The expression of differentiation markers of TAK1-KO epidermis at P0 was similar to that of controls. The expression pattern started to change at P2, and the changes became more marked at P6. The expression of K5 and K14 is normally confined to the basal cell layer, as seen in the control. However, the suprabasal keratinocytes of TAK1-KO mice at P6 expressed K5 and K14. K1, K10, and loricrin are markers for the suprabasal and late phase differentiation of keratinocytes and are normally expressed on the suprabasal keratinocytes and in the upper epidermis, respectively. In addition to the ectopic expression of K5 and K14, the expression of K1, K10, and loricrin was absent on the viable epidermal keratinocytes of TAK1-KO mice at P6. Furthermore, the epidermis of TAK1-KO mice at P6 expressed K16, a marker for inflammatory and hyperproliferative epidermal keratinocytes; K16 expression was absent from control mice. These data indicate that keratinocyte differentiation was disturbed by removing TAK1 from keratinocytes.

We further analyzed growth and apoptosis in the epidermis using Ki67 staining and the TUNEL method (Fig. 5). The staining of Ki67 revealed increased proliferation of keratinocytes in the epidermis of TAK1-KO mice at P6 (Fig. 5*A*), in contrast to the increased apoptosis shown with the TUNEL method (Fig. 5*B*). Furthermore, Ki67-positive keratinocytes were present in the suprabasal layer of the epidermis of TAK1-KO mice. The expression of p50 and p65 in the basal layer of the epidermis of TAK1-KO mice was decreased at P6 (Fig. 5*C*).

Induction of K1 in the Keratinocytes of TAK1-KO Mice in Suspension Culture—Based on the immunohistochemical results, we postulated that the keratinocytes of TAK1-KO mice do not express K1 by differentiation. To test this, we isolated and cultured keratinocytes from the epidermis of newborn mice. Although the number of Ki67-positive keratinocytes was increased in the epidermis of TAK1-KO mice, the *in vitro* growth of keratinocytes obtained from TAK1-KO mice was significantly reduced. Therefore, to study the ability of keratinocytes to differentiate, freshly isolated keratinocytes were seeded on culture plates and incubated overnight; adherent cells were subjected to suspension culture (3) to induce differentiation. Unexpectedly, the keratinocytes from TAK1-KO mice induced K1 in the suspension culture, as did those from control mice (Fig. 6).

Apoptosis of Keratinocytes on Depletion of TAK1 in Culture—Because of the difficulty in culturing TAK1-KO keratinocytes, we depleted TAK1 in cultured keratinocytes obtained from the control mice (*Map3k7*$^{flox/flox}$). An adenovirus vector carrying Cre-recombinase (Ax-Cre) was transfected to the cultured keratinocytes. Empty Ax-1W vector was used as a control. As shown in Fig. 7, the expression of TAK1 was reduced to 0.4-fold that in control mice at 48 h after the transfection of Ax-Cre. The reduction of TAK1 in cultured keratinocytes resulted in apo-

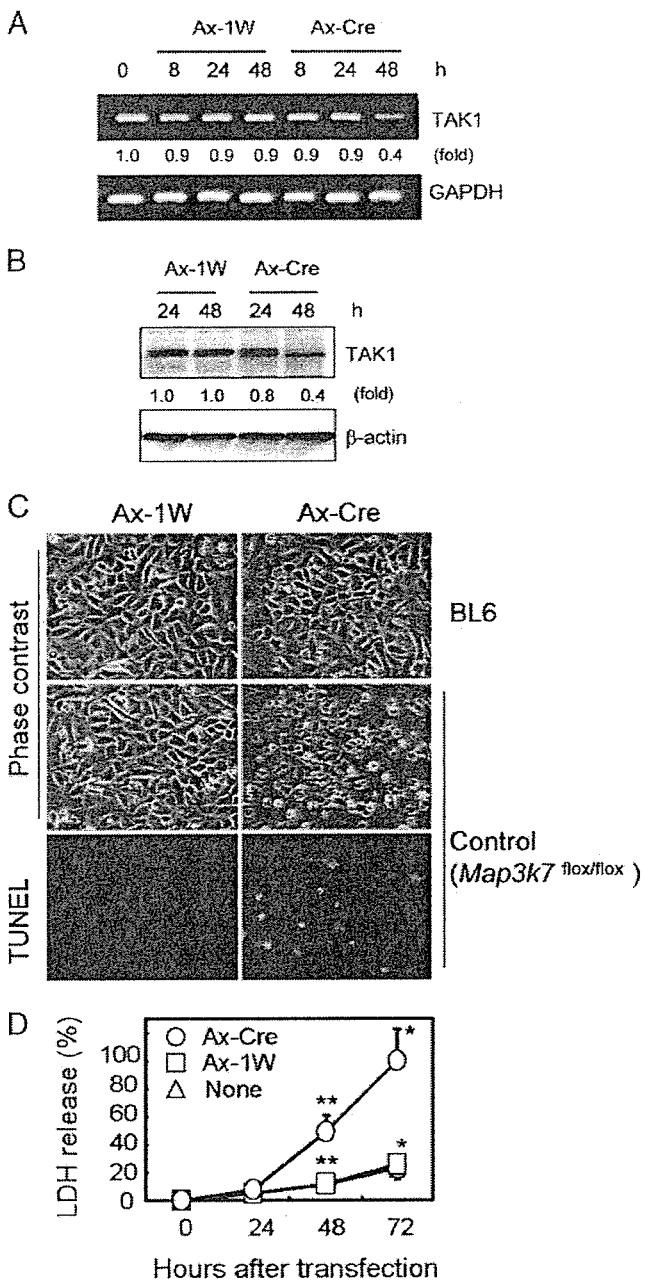

FIGURE 7. **Apoptosis on depletion of TAK1 from cultured keratinocytes.** TAK1 expression was depleted in cultured keratinocytes of the control mice (*Map3k7*$^{flox/flox}$). An adenovirus vector carrying Cre-recombinase (Ax-Cre) was transfected into the cultured keratinocytes at a multiplicity of infection of 100. The empty vector Ax-1W was used for the control. The expression of TAK1 mRNA and protein were analyzed using RT-PCR (*A*) and Western blotting (*B*). The intensity of each band was quantified relative to the control, set at one unit. Glyceraldehyde-3-phosphate dehydrogenase and β-actin are internal standards. There was a weak band in the cells treated with Ax-Cre that was slightly lower than that of Ax-1W at 48 h (*B*). This might represent TAK1Δ (15), as in Fig. 1*E*. At 72 h after transfection, the cell morphology was observed under a phase contrast microscope, and apoptotic cells were detected using the TUNEL method (*C*). Keratinocytes of C57/BL6 (BL6) mice were also transfected with Ax vector as a control. Cell death was quantified by measuring LDH release (*D*). Ax was transfected to the cultured keratinocytes, and the culture supernatant was harvested for LDH assay at the indicated time. LDH release was expressed as the percentage of total LDH (mean ± S.E.), which was obtained by summing the LDH release and the LDH of living cells. The statistical significance was determined using the paired Student's *t* test ($n = 5$). * and **, differences were considered statistically significant for $p < 0.01$.

ptosis 72 h after transfection (Fig. 7*C*), indicating that TAK1 prevents keratinocyte apoptosis. The quantitative analysis of cell death based on measurements of LDH release revealed that the apoptosis started at 48 h and was completed at 72 h (*D*).

DISCUSSION

Although TAK1 is evolutionarily conserved and is thought to be an important intracellular signaling molecule, little is known about its physiological roles. In *Xenopus* embryonic development, TAK1 is involved in mesoderm induction mediated by bone morphogenetic protein, a member of the transforming growth factor β family (18). TAK1-deficient *Drosophila* are viable and fertile, but they do not produce antibacterial peptides and are highly susceptible to Gram-negative bacteria infection (19). In HeLa cells, it is thought that TAK1 is involved in the TNF receptor and IL-1 receptor/Toll-like receptor-mediated signaling pathways upstream from NF-κB and MAPKs, based on small interfering RNA inhibition of TAK1 expression (11). Because TAK1-deficient mice are embryonically lethal (15), by utilizing embryonic fibroblasts, a loss of response to IL-1β and TNF in TAK1-deficient cells was demonstrated (15). To study the role of TAK1 in B cell function, mice with B cell-specific TAK1 deficiency were generated (15). The B cell-specific TAK1-deficient mouse showed that TAK1 was indispensable for B cell activation in response to Toll-like receptor ligands (CpG DNA, poly(I:C), and LPS), CD40, and B cell receptor cross-linking (15). Furthermore, TAK1-deficient B cells failed to activate NF-κB and JNK in response to IL-1β, TNF, and Toll-like receptor ligands. Therefore, TAK1 has essential functions in the Toll-like receptor-, IL-1 receptor-, TNF receptor-, and B cell receptor-mediated cellular responses. In addition, we showed that TAK1 is essential for regulating keratinocyte differentiation and preventing keratinocyte apoptosis in the epidermis.

TAK1-KO mice die by P7. Because the barrier function of the epidermis was severely disturbed, as shown by TEWL, the impaired homeostasis of body fluids resulting from water loss through the skin may have caused the early mortality. Another possible cause of the early mortality is impaired feeding. The body weight at death was approximately half that of the control mice. The lips of the TAK1-KO mice showed signs of scaling, and the histological study revealed massive keratinocyte apoptosis (data not shown), as in the oral mucosa. These findings suggested that the diseased lip and oral mucosa affected nursing, resulting in severe growth retardation, which might cause the early mortality.

TAB1 and TAB2 were identified as adaptor proteins of TAK1 using yeast two-hybrid screening (10, 13). TAB1 binds to TAK1 constitutively and induces kinase activity on stimulation with IL-1. TAB2 is an adaptor molecule linking TRAF6 and TAK1. With IL-1 stimulation, TAB2 translocates from the cell membrane to the cytosol and binds to TRAF6 and TAK1. TAB3 is a TAB2 homologue that interacts with TRAF6 and TRAF2 on stimulation with IL-1 and TNF, respectively (12). Co-transfection with small interfering RNA s directed against both TAB2 and TAB3 inhibited both the IL-1- and TNF-induced activation of TAK1 and NF-κB (12). These results suggest that TAB2 and TAB3 play redundant roles as mediators of TAK1 activation in IL-1 and TNF signal transduction. Although TABs have been

identified as TAK1 adaptor proteins, the genetic study of these proteins suggested that they do not always function together as a TAK1 complex. The neural tube development was abnormal in the TAK1-deficient embryo (20). This phenotype is substantially different from those of TAB1-deficient (abnormal cardiovascular and pulmonary morphogenesis) and TAB2-deficient (liver degeneration and apoptosis) mice (21, 22). These data suggested not only that TAK1 and the TAB complex function as a single unit, but that each component has a distinct role during development (20). Furthermore, the roles of TABs in keratinocytes have not yet been studied. Therefore, molecular interaction between TABs and TAK1 and their roles in keratinocytes should be clarified.

Genetic studies have shown that mutations in the human *NEMO/IKK-γ* gene are the cause of incontinentia pigmenti or Bloch-Sulzberger syndrome (23). Disruption of the *NEMO/IKK-γ* gene causes female mice to develop patchy skin lesions with massive granulocyte infiltration and hyperproliferation and increased apoptosis of keratinocytes (24, 25). Diseased animals show severe growth retardation and early mortality (24, 25). Although the skin lesion of TAK1-KO mice was not patchy, the clinical appearance, histological findings, and early mortality were similar to those in IKK-γ deficiency. The formation of patchy lesions in IKK-γ deficiency is thought to be the result of a chimerism in the IKK-γ-deficient mouse. Furthermore, the epidermis-specific deletion of IKK-β/IKK2 increased apoptosis and the abnormal expression of differentiation markers, including K6, K14, K10, and loricrin (26), resembling the characteristics of TAK1-KO mice. The development of similar skin phenotypes among mice with TAK1-, IKK-β-, or IKK-γ-deficient epidermal keratinocytes indicates the disruption of a common pathway in these mice. Given that TAK1 activates the IKK complex, the signal from TAK1 to NF-κB might be disrupted in the IKK-β- or IKK-γ-deficient epidermis.

Although apoptosis was almost 100% at 72 h in Fig. 7*D*, TAK1 expression was still 0.4-fold 48 h after Ax-Cre transfection (Fig. 7, *A* and *B*). There are three possibilities for this discrepancy: 1) The band in the Western blot of cells transfected with Ax-Cre was slightly lower than that of Ax-1W at 48 h (B); this may represent TAK1Δ, which lacks the ATP-binding site required for kinase activity (15), as in Fig. 1*E*. Therefore, the active TAK1 has already disappeared, and a small amount of inactive TAK1 (TAK1Δ) appeared instead. 2) Cells started to die 48 h after Ax-Cre transfection. Because the dead cells detached spontaneously or on washing the culture dishes, and only living cells were subjected to analysis, it is most likely that cells expressing 0.4-fold TAK1 were still alive, whereas the complete loss of TAK1 had resulted in the apoptosis of cells that were not included in the analysis. At 72 h, TAK1 knockdown may be complete, and all the cells underwent apoptosis. 3) The transfection efficiency of Ax-Cre might not be equal for all cells. In less transfected cells, TAK1 expression might not be reduced. This might cause the 0.4-fold TAK1 expression at 48 h. Moreover, the high expression of Cre caused the complete loss of TAK1 and apoptosis at 48 h, but these cells were not included in the analysis, as discussed in the second possible explanation. One reason or a combination of these reasons might cause this discrepancy.

A possible role for NF-κB in negative cellular growth control via cell cycle regulation has been suggested (1, 5, 6). Growth inhibitory genes are induced by p65 in keratinocytes but not in other cell types (27). In the p65-deficient mouse, the number of Ki67-positive keratinocytes increased in the epidermis, and keratinocyte proliferation increased in culture (4). Based on the increased number of Ki67-positive cells in TAK1-KO mice seen in this study, we postulate that cell growth increased. However, the proliferation of TAK1-KO keratinocytes is reduced *in vitro*. IKK-β-deficient keratinocytes are also hypoproliferative *in vitro*, despite an increased number of Ki67-positive cells in the epidermis (26). One possible mechanism to account for an increased number of Ki67-positive cells and decreased proliferation *in vitro* is the induction of apoptosis that overtakes proliferation. However, this cannot explain the discrepancy between TAK1 and IKK-β deficiencies and p65 deficiency. Similar phenotypic discrepancy has also been found between IKKα/IKK1-deficient mice and others; the phenotypes of IKKα-deficient mice are somewhat different from those of mice deficient in p65, IκB kinase 2, or IKKβ. Mice lacking IKKα died perinatally and showed severely impaired limb outgrowth and abnormal epidermal differentiation (28, 29). These results suggest that the phenotypic differences among these deficient mice result from the loss of individual upstream signaling molecules of NF-κB that do not completely impair NF-κB function.

The loss of adhesion to the extracellular matrix in suspension culture strongly induces keratinocyte differentiation (3). Although the epidermis of TAK1-KO mice showed abnormal differentiation, the keratinocytes of TAK1-KO mice differentiated to express K1 in suspension culture. Similarly, IKK-β-deleted keratinocytes retained the ability to differentiate in suspension culture despite the failure of epidermal differentiation (26). These data indicate that the regulation of keratinocyte differentiation by TAK1 and IKK-β is independent of the initiation of differentiation by the loss of adhesion to the extracellular matrix.

Keratinocytes in the basal cell layer of control mice expressed p50 and p65, whereas the expression of p50 and p65 in the basal cell layer of TAK1-KO mice was decreased. One possible cause of the decreased expression is abnormal differentiation. High expression levels of p50 and p65 are normally found in the keratinocytes of the basal layer. However, the keratinocytes in the TAK1-KO basal layer did not possess a characteristic feature of the basal layer, the expression of K5 and K14. This abnormal differentiation might cause decreased expression of p50 and p65. As a result of decreased p50 and p65 expression, the NF-κB signal is scarcely transduced to the downstream signaling pathway, in addition to the lack of TAK1. In conclusion, TAK1 is essential in regulating keratinocyte growth, differentiation, and apoptosis.

Acknowledgments—We thank Teruko Tsuda and Eriko Tan for providing significant technical assistance.

REFERENCES

1. Seitz, C. S., Lin, Q., Deng, H., and Khavari, P. A. (1998) *Proc. Natl. Acad. Sci. U. S. A.* **95**, 2307–2312
2. Sayama, K., Hanakawa, Y., Shirakata, Y., Yamasaki, K., Sawada, Y., Sun, L., Yamanishi, K., Ichijo, H., and Hashimoto, K. (2001) *J. Biol. Chem.* **276**,

999–1004
3. Sayama, K., Yamasaki, K., Hanakawa, Y., Shirakata, Y., Tokumaru, S., Ijuin, T., Takenawa, T., and Hashimoto, K. (2002) *J. Biol. Chem.* **277,** 40390–40396
4. Zhang, J. Y., Green, C. L., Tao, S., and Khavari, P. A. (2004) *Genes Dev.* **18,** 17–22
5. Seitz, C. S., Deng, H., Hinata, K., Lin, Q., and Khavari, P. A. (2000) *Cancer Res.* **60,** 4085–4092
6. Dajee, M., Lazarov, M., Zhang, J. Y., Cai, T., Green, C. L., Russell, A. J., Marinkovich, M. P., Tao, S., Lin, Q., Kubo, Y., and Khavari, P. A. (2003) *Nature* **421,** 639–643
7. Zhang, J. Y., Tao, S., Kimmel, R., and Khavari, P. A. (2005) *J. Cell Biol.* **168,** 561–566
8. Seitz, C. S., Freiberg, R. A., Hinata, K., and Khavari, P. A. (2000) *J. Clin. Investig.* **105,** 253–260
9. Yamaguchi, K., Shirakabe, K., Shibuya, H., Irie, K., Oishi, I., Ueno, N., Taniguchi, T., Nishida, E., and Matsumoto, K. (1995) *Science* **270,** 2008–2011
10. Takaesu, G., Kishida, S., Hiyama, A., Yamaguchi, K., Shibuya, H., Irie, K., Ninomiya-Tsuji, J., and Matsumoto, K. (2000) *Mol. Cell* **5,** 649–658
11. Takaesu, G., Surabhi, R. M., Park, K. J., Ninomiya-Tsuji, J., Matsumoto, K., and Gaynor, R. B. (2003) *J. Mol. Biol.* **326,** 105–115
12. Ishitani, T., Takaesu, G., Ninomiya-Tsuji, J., Shibuya, H., Gaynor, R. B., and Matsumoto, K. (2003) *EMBO J.* **22,** 6277–6288
13. Shibuya, H., Yamaguchi, K., Shirakabe, K., Tonegawa, A., Gotoh, Y., Ueno, N., Irie, K., Nishida, E., and Matsumoto, K. (1996) *Science* **272,** 1179–1182
14. Cheung, P. C., Nebreda, A. R., and Cohen, P. (2004) *Biochem. J.* **378,** 27–34
15. Sato, S., Sanjo, H., Takeda, K., Ninomiya-Tsuji, J., Yamamoto, M., Kawai, T., Matsumoto, K., Takeuchi, O., and Akira, S. (2005) *Nat. Immunol.* **6,** 1087–1095
16. Takeda, J., Sano, S., Tarutani, M., Umeda, J., and Kondoh, G. (2000) *J Dermatol. Sci.* **23,** 147–154
17. Hanakawa, Y., Amagai, M., Shirakata, Y., Sayama, K., and Hashimoto, K. (2000) *J. Cell Sci.* **113,** 1803–1811
18. Shibuya, H., Iwata, H., Masuyama, N., Gotoh, Y., Yamaguchi, K., Irie, K., Matsumoto, K., Nishida, E., and Ueno, N. (1998) *EMBO J.* **17,** 1019–1028
19. Vidal, S., Khush, R. S., Leulier, F., Tzou, P., Nakamura, M., and Lemaitre, B. (2001) *Genes Dev.* **15,** 1900–1912
20. Shim, J. H., Xiao, C., Paschal, A. E., Bailey, S. T., Rao, P., Hayden, M. S., Lee, K. Y., Bussey, C., Steckel, M., Tanaka, N., Yamada, G., Akira, S., Matsumoto, K., and Ghosh, S. (2005) *Genes Dev.* **19,** 2668–2681
21. Komatsu, Y., Shibuya, H., Takeda, N., Ninomiya-Tsuji, J., Yasui, T., Miyado, K., Sekimoto, T., Ueno, N., Matsumoto, K., and Yamada, G. (2002) *Mech. Dev.* **119,** 239–249
22. Sanjo, H., Takeda, K., Tsujimura, T., Ninomiya-Tsuji, J., Matsumoto, K., and Akira, S. (2003) *Mol. Cell. Biol.* **23,** 1231–1238
23. Smahi, A., Courtois, G., Vabres, P., Yamaoka, S., Heuertz, S., Munnich, A., Israel, A., Heiss, N. S., Klauck, S. M., Kioschis, P., Wiemann, S., Poustka, A., Esposito, T., Bardaro, T., Gianfrancesco, F., Ciccodicola, A., D'Urso, M., Woffendin, H., Jakins, T., Donnai, D., Stewart, H., Kenwrick, S. J., Aradhya, S., Yamagata, T., Levy, M., Lewis, R. A., and Nelson, D. L. (2000) *Nature* **405,** 466–472
24. Schmidt-Supprian, M., Bloch, W., Courtois, G., Addicks, K., Israel, A., Rajewsky, K., and Pasparakis, M. (2000) *Mol. Cell* **5,** 981–992
25. Makris, C., Godfrey, V. L., Krahn-Senftleben, G., Takahashi, T., Roberts, J. L., Schwarz, T., Feng, L., Johnson, R. S., and Karin, M. (2000) *Mol. Cell* **5,** 969–979
26. Pasparakis, M., Courtois, G., Hafner, M., Schmidt-Supprian, M., Nenci, A., Toksoy, A., Krampert, M., Goebeler, M., Gillitzer, R., Israel, A., Krieg, T., Rajewsky, K., and Haase, I. (2002) *Nature* **417,** 861–866
27. Hinata, K., Gervin, A. M., Jennifer Zhang, Y., and Khavari, P. A. (2003) *Oncogene* **22,** 1955–1964
28. Takeda, K., Takeuchi, O., Tsujimura, T., Itami, S., Adachi, O., Kawai, T., Sanjo, H., Yoshikawa, K., Terada, N., and Akira, S. (1999) *Science* **284,** 313–316
29. Hu, Y., Baud, V., Delhase, M., Zhang, P., Deerinck, T., Ellisman, M., Johnson, R., and Karin, M. (1999) *Science* **284,** 316–320

Oncogene (2007) 26, 339–348

www.nature.com/onc

ORIGINAL ARTICLE

Pre-B-cell leukemia transcription factor 1 is a major target of promyelocytic leukemia zinc-finger-mediated melanoma cell growth suppression

K Shiraishi[1,2], K Yamasaki[2], D Nanba[1], H Inoue[1], Y Hanakawa[2], Y Shirakata[2], K Hashimoto[2] and S Higashiyama[1,3]

[1]*Department of Biochemistry and Molecular Genetics, Ehime University Graduate School of Medicine, Shitsukawa, Toon, Ehime, Japan;* [2]*Department of Dermatology, Ehime University Graduate School of Medicine, Shitsukawa, Toon, Ehime, Japan and* [3]*Precursory Research for Embryonic Science and Technology (PRESTO), Japan Science and Technology Corporation (JST), Kawaguchi City, Saitama, Japan*

Promyelocytic leukemia zinc-finger (PLZF) is a transcriptional repressor and tumor suppressor. PLZF is expressed in melanocytes but not in melanoma cells, and recovery of PLZF expression markedly suppresses melanoma cell growth. Several target genes regulated by PLZF have been identified, but the precise function of PLZF remains uncertain. Here, we searched for candidate target genes of PLZF by DNA microarray analysis. Pre-B-cell leukemia transcription factor 1 (Pbx1) was one of the prominently suppressed genes. Pbx1 was highly expressed in melanoma cells, and its expression was reduced by transduction with the PLZF gene. Moreover, the growth suppression mediated by PLZF was reversed by enforced expression of Pbx1. Knockdown of Pbx1 by specific small interfering RNAs suppressed melanoma cell growth. We also found that Pbx1 binds HoxB7. Reverse transcription–polymerase chain reaction analysis demonstrated that repression of Pbx1 by PLZF reduces the expression of HoxB7 target genes, including tumor-associated neoangiogenesis factors such as basic fibroblast growth factor, angiopoietin-2 and matrix metalloprotease 9. These findings suggest that deregulation of Pbx1 expression owing to loss of PLZF expression contributes to the progression and/or pathogenesis of melanoma.
Oncogene (2007) **26**, 339–348. doi:10.1038/sj.onc.1209800; published online 24 July 2006

Keywords: Pbx1; PLZF; Hox; melanoma

Introduction

Malignant melanoma is a highly aggressive neoplastic disease whose incidence is increasing rapidly. To develop new therapies, it is essential to elucidate the molecular mechanisms by which melanocytes are transformed into malignant melanoma cells. A recent report found that the promyelocytic leukemia zinc-finger (PLZF) protein is expressed in melanocytes but not in melanoma cells, and that melanoma growth is markedly suppressed by enforced expression of PLZF (Felicetti *et al.*, 2004).

PLZF was first identified by its translocation with retinoic acid receptor alpha in t(11;17) acute promyelocytic leukemia (Chen *et al.*, 1993). The PLZF protein is a sequence-specific transcription repressor characterized by a BTB/POZ domain, which is responsible for transcriptional repression, and nine zinc-finger domains that form the DNA-binding domain (Hong *et al.*, 1997; Li *et al.*, 1997; Wong and Privalsky, 1998). Some target genes regulated by PLZF have been identified. Studies of PLZF-knockout mice indicate that PLZF represses HoxD gene expression through chromatin remodeling, which in turn regulates limb and axial skeletal patterning (Barna *et al.*, 2000, 2002). PLZF also binds to and represses the cyclin A2 promoter, and is involved in the regulation of cell cycle progression (Yeyati *et al.*, 1999). Moreover, PLZF represses c-*myc* expression, which is central to the control of cellular proliferation, apoptosis and differentiation (McConnell *et al.*, 2003). DNA microarray analyses have also revealed numerous candidate genes targeted by PLZF (McConnell *et al.*, 2003; Costoya *et al.*, 2004; Felicetti *et al.*, 2004). These target genes may have a great influence on the progression of melanoma, but their role in the aggressiveness of this cancer remains unknown.

For this reason, we used DNA microarray analysis to search for additional PLZF target genes. One of the most strongly regulated genes identified was pre-B-cell leukemia transcription factor 1 (Pbx1). Pbx1 is also a transcriptional regulator and a binding partner for a number of Hox proteins (Mann and Chan, 1996; Shanmugam *et al.*, 1997). We confirmed that Pbx1 is highly expressed in melanoma cells and that cell growth is markedly suppressed when its expression is knocked down. Furthermore, we identified HoxB7 as a binding

Correspondence: Dr S Higashiyama, Department of Biochemistry and Molecular Genetics, Ehime University Graduate School of Medicine, Shitsukawa, Toon, Ehime 791-0295, Japan.
E-mail: shigeki@m.ehime-u.ac.jp
Received 1 November 2005; revised 30 May 2006; accepted 31 May 2006; published online 24 July 2006

partner of Pbx1 in melanoma cells. We show here that PLZF suppresses the expression of Pbx1-HoxB7 target genes as well as Pbx1 itself and that dysregulation of this network owing to loss of PLZF may play an important role in the progression of melanoma.

Results

PLZF suppresses Pbx1 gene expression

Felicetti *et al.* (2004) reported that primary melanomas and melanoma cell lines completely lack PLZF gene expression and that enforced expression of PLZF in melanoma cell lines suppressed their growth *in vitro* and *in vivo*. We confirmed these results using 15 melanoma cell lines, including A375, 397 cell lines and their PLZF transfectants (data not shown).

We then examined which genes are repressed by PLZF in the melanoma cells by DNA microarray analysis. For these experiments, we constructed adenovirus vectors carrying the genes encoding PLZF and LacZ and used them to infect A375 and 397 cells at a multiplicity of infection (MOI) of 200. Several genes exhibited different levels of expression in PLZF-negative and PLZF-positive cells. We found that Pbx1 was the most prominently downregulated transcription factor in PLZF-positive cells (Table 1). Reverse transcription–polymerase chain reaction (RT–PCR) confirmed that Pbx1 mRNA expression in A375 cells was clearly and substantially reduced in a time-dependent manner after infection with the PLZF adenovirus (Figure 1a). The expression of Pbx1 mRNA decreased to 25% of that in LacZ-infected cells. In addition, the Pbx1 protein levels in the PLZF-infected cells decreased by approximately 40% when compared with cells infected with the LacZ adenovirus or non-infected cells (Figure 1b). We also obtained similar results in 397 cells.

Enforced expression of Pbx1 rescues growth suppression by PLZF

In order to determine the relative importance of PLZF-mediated downregulation of Pbx1 in the growth of melanoma cells, we examined the proliferation of stable PLZF-expressing melanoma cells transfected with the pME18S-Pbx1 or pME18S control vector. Pbx1 protein levels in the transfected cells were first estimated by Western blotting (Figure 2a). Pbx1 levels increased approximately 1.5- and 1.3-fold in A375P and A375 cells, respectively, in comparison with controls. We also examined transfection efficiency in these cells using the mixture of pME18S-Pbx1 and pME18S-ECFP (Enhanced Cyan Fluorescent Protein) vectors. We found that approximately 65% of the cells were CFP (Cyan Fluorescent Protein)-positive (Figure 2b, inset). We then investigated the growth of A375 and A375P cells after transient transfection with pME18S-Pbx1 or pME18S. Exogenous expression of Pbx1 did not cause further enhancement of A375 cell growth. This suggests that there was sufficient endogenous Pbx1 expression. A375P cells exhibited a marked downregulation of both endogenous Pbx1 expression and cell growth. This effect was partially (approximately 40%) rescued by the expression of exogenous Pbx1 (Figure 2b), thus suggesting the presence of a Pbx1-independent pathway in PLZF-transfected melanoma cells. We also obtained similar results in 397 and 397P cells (data not shown).

Table 1 Expression profile obtained by array hybridization

Genes[a]	*Description*	*Accession number*	*Ratio (PLF/LacZ)*	
tzfp	Testis zinc-finger protein	NM_014383	Up	> × 20
pnkp	Polynucleotide kinase 3′-phosphatase	NM_007254	Up	
mapk4	Mitogen-activated protein kinase 4	XM_008806	Up	
oas3	2′–5′ Oligoadenylate synthetase 3	NM_006187	Up	× 10– × 20
osmr	Oncostatin m receptor	NM_003999	Up	
fezl	Zygin I, isoform 1	NM 005103	Up	
tssc3	Tumor-suppressing subtransferable candidate 3	NM 003311	Up	
lmo6	Linn domain-only 6	NML006150	Up	
nfsl	Nfsl nitrogen fixation 1	NM_021100	Up	× 5– × 10
cir	Ebfl-interacting corepressor	NM_004882	Up	
btebl	Basic transcription element-binding protein 1	NM_001206	Up	
netl	P65 netl proto-oncogene protein	S82401	Down	< × 0.05
cacng7	Calcium channel gamma subunit 7	AF2S8387	Down	× 0.05– × 0.1
rgs6	Regulator of g-protein signalling 6	NM 004296	Down	
pbxl	Pre-B-cell leukemia transcription factor 1	NM_002585	Down	× 0.1– × 0.2
calbl	Calbindinl	NM_004929	Down	
arhgdig	rho gdp dissociation inhibitor gamma	NM_001176	Down	
chrna 10	Cholinergic receptor, alpha polypeptide 10	NM_020402	Down	
hgc6.2	Hgc6.2 protein	NM_014356	Down	
dc20	Dc20	AF311338	Down	
serpinhl	Serine proteinase inhibitor, clade h, member 1	NM_004353	Down	

Adenoviral transduction of PLZF was chosen for expressing PLZF in A375 and 397 cells instead of stably expressing of PLZF, because of (1) avoiding the bias of cell response for PLZF by cloning of drug-resistant cells and (2) controlling the expression level of PLZF. The levels of HoxB7, bFGF, Ang-2 and MMP9 were in the range of × 0.25– × 0.5. [a]These genes were common in both A375 and 397 cells in duplicate microarray analyses.

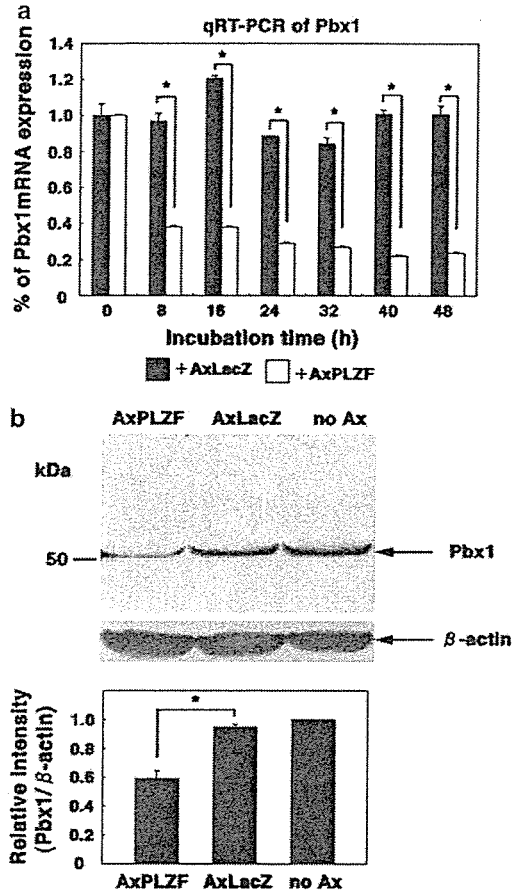

Figure 1 PLZF suppresses Pbx1 gene expression. (a) qRT–PCR of Pbx1 mRNA in A375 cells infected with LacZ or PLZF adenovirus. $^*P<0.05$. (b) Upper panel: Western blot analysis of Pbx1 protein in A375 cells infected with LacZ or PLZF adenovirus and in uninfected cells. Lower panel: Relative intensity of Pbx1 proteins calculated as a ratio vs expression of β-actin. $^*P<0.05$. AxLacZ, infection with LacZ adenovirus (MOI 200); AxPLZF, infection with PLZF adenovirus (MOI 200); no Ax, no infection. Each experiment was performed in duplicate.

PLZF physically interacts with the Pbx1 promoter

In order to demonstrate direct regulation of the Pbx1 gene by PLZF, we searched the Pbx1 promoter for a putative PLZF-binding site using the TFSEARCH program (Heinemeyer *et al.*, 1998, http://mbs.cbrc.jp/research/db/TFSERCHJ.html), which suggested seven potential PLZF DNA recognition sequences located within a 3.0-kb region upstream of the transcription initiation site (Figure 3a). We then used a 3.0-kb fragment of the Pbx1 promoter in a reporter assay. The luciferase activity of Pbx1–3.0 was markedly suppressed in A375P, as compared to A375 cells (Figure 3b). Electrophoretic mobility shift assay (EMSA) was subsequently performed with nuclear extracts made from A375 cells infected with PLZF adenovirus and uninfected cells in order to identify the PLZF DNA recognition site in the Pbx1 promoter. Site 1 (2998 bp upstream) and Site 4 (2433 bp upstream) bound with factors in the A375 cell extracts without

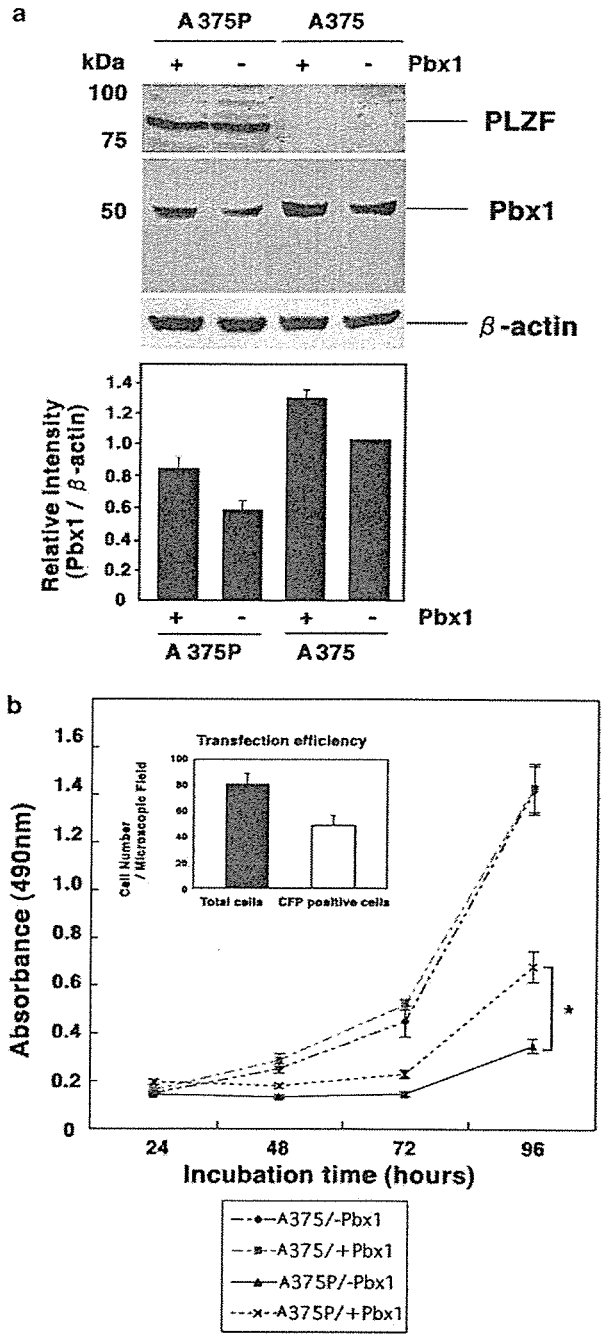

Figure 2 Enforced expression of Pbx1 rescues growth suppression of melanoma cells by PLZF. (a) Upper panel: Western blot analysis of PLZF and Pbx1 in A375 and A375P cells transfected with PME18S-Pbx1 or PME18S control vector. Lower panel: Relative intensity of Pbx1 protein, which was calculated as the ratio of Pbx1 vs β-actin. (b) Growth curves of A375 and A375P cells transfected with PME18S-Pbx1 and PME18S control vector. $^*P<0.05$. Inset: Transfection efficiency of pME18S-Pbx1 was evaluated by counting CFP-positive cells transfected with both PME18S-Pbx1 and pME18S-ECFP.

PLZF expression (stars in lane 1 and lane 7), and formed another complex in the A375 cell extracts expressing PLZF (arrow in lane 2, Figure 3c). On the other hand,

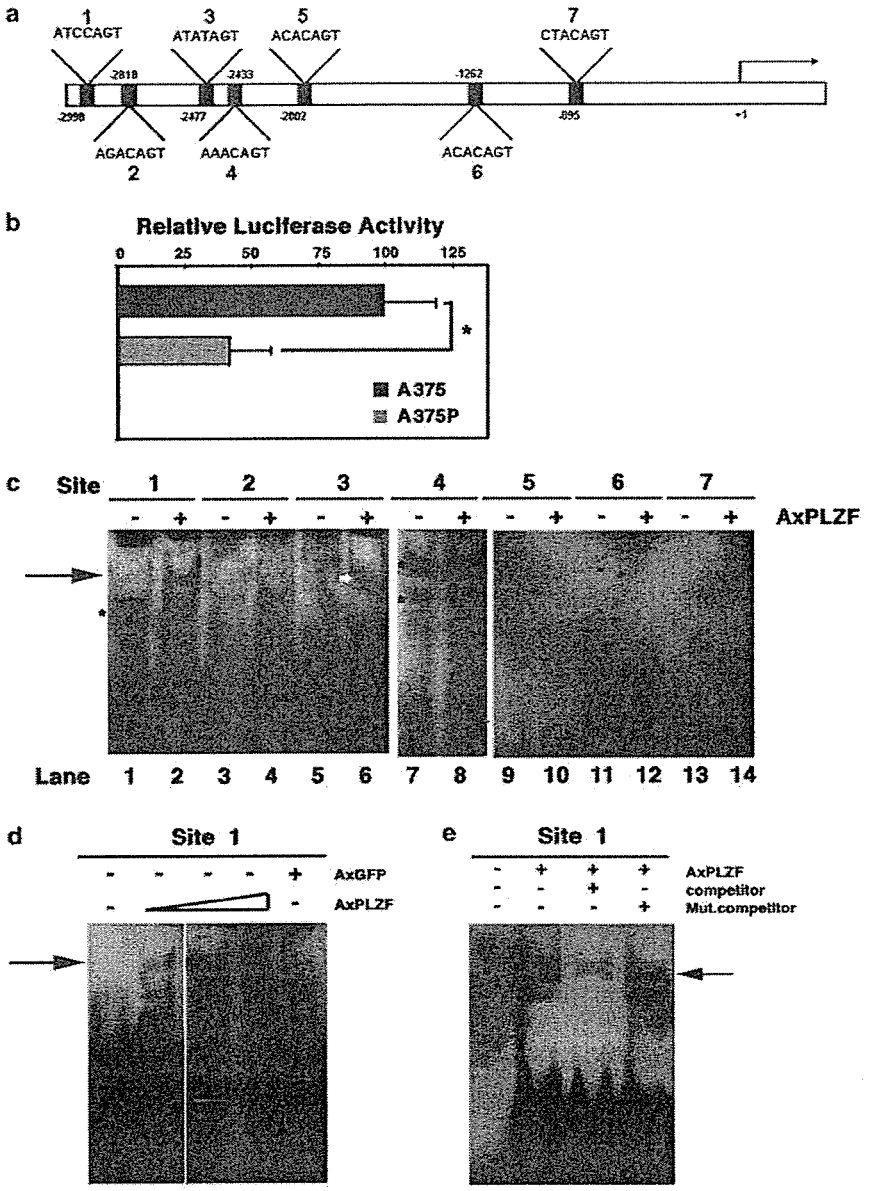

Figure 3 PLZF protein directly interacts with the Pbx1 promoter. (**a**) Schematic depiction of the Pbx1 promoter region and seven potential binding sites for PLZF (Sites 1–7). The +1 position corresponds to the initiation site of transcription. (**b**) Relative luciferase activity measured at 24 h after transfection of pGL Pbx1–3.0 into A375 cells and A375P cells. Each experiment was performed in triplicate and data represent the means ± s.d. of three independent experiments. (**c**) EMSA carried out with nuclear extracts of A375 cells infected with PLZF adenovirus (MOI 100) and uninfected cells. White arrowhead in lane 6 shows stain. (**d**) Specificity of interaction between PLZF and Site 1 (an arrow) was confirmed by EMSA using nuclear extracts of A375 cells infected with PLZF (MOI 50, 100 and 200) or GFP adenovirus (MOI 200). (**e**) Interaction between PLZF and Site 1 (an arrow) was found to compete with unlabeled Site 1 but not with unlabeled mut. Site 1.

Sites 2, 3, 4, 5, 6 and 7 did not form additional complexes in the A375 cell extracts expressing PLZF, as compared to A375 cell extracts without PLZF (lanes 3–14, see comments on lane 6 in figure legends). To confirm the specificity of the interaction between Site 1 and PLZF, we carried out dose–response analysis and competition analysis. The interaction between Site 1 and PLZF exhibited a dose-dependent relationship (Figure 3d), and was completely abolished by the addition of the competitor (unlabeled Site 1). The competitor with the mutation (mutated Site 1, see 'Materials and methods') failed to abolish the PLZF–Site 1 interaction (Figure 3e). On the other hand, deletion of Site 1 from Pbx1–3.0 (Pbx1–3.0/ΔSite 1) did not show significant recovery of Pbx1 promoter activity (data not shown), indicating that Site 1 is an interactive site for PLZF, and is not sufficient for complete repression of Pbx1 gene expression. These results

suggest that repression of Pbx1 gene expression by PLZF is regulated by multiply direct and/or indirect mechanisms.

Melanoma cell growth is suppressed by Pbx1 small interfering RNAs

In order to further characterize the role of Pbx1 in melanoma cell growth, we examined the suppression of melanoma cell growth by Pbx1 knockdown using two types of small interfering RNA (siRNA) (siRNA1 and siRNA2). Mutated siRNAs (mut. siRNA1 and mut. siRNA2) were used as controls. We confirmed that transfection of A375 and 397 cells with Pbx1 siRNA1 significantly reduced Pbx1 mRNA (data not shown) and protein levels (Figure 4a). In addition, transfection of A375 and 397 cells with Pbx1 siRNA1, but not Pbx1 mut. siRNA1, caused marked and statistically significant suppression of cell growth (Figure 4b). These data suggest that Pbx1 is involved in cell growth of A375 and 397 cells. siRNA2 showed similar results as siRNA1 (data not shown).

Pbx1 binds HoxB7

Pbx1 forms complexes with a number of Hox proteins, and HoxB7 was expressed strongly in all melanoma cell lines tested (Care *et al*., 1996). We investigated whether Pbx1 interacts with HoxB7 in A375 and 397 cells. HoxB7 was immunoprecipitated from cell lysates and was then analysed by immunoblotting with anti-Pbx1 antibody. We detected a 52-kDa band corresponding to Pbx1 in both cell lines (Figure 5). We also found that an anti-Pbx1 antibody co-immunoprecipitated HoxB7 from the same cell lysates (data not shown).

Expression of HoxB7 target genes is downregulated by reduction of Pbx1

We investigated the effects of Pbx1 knockdown on the expression of HoxB7 and its target genes. Knockdown

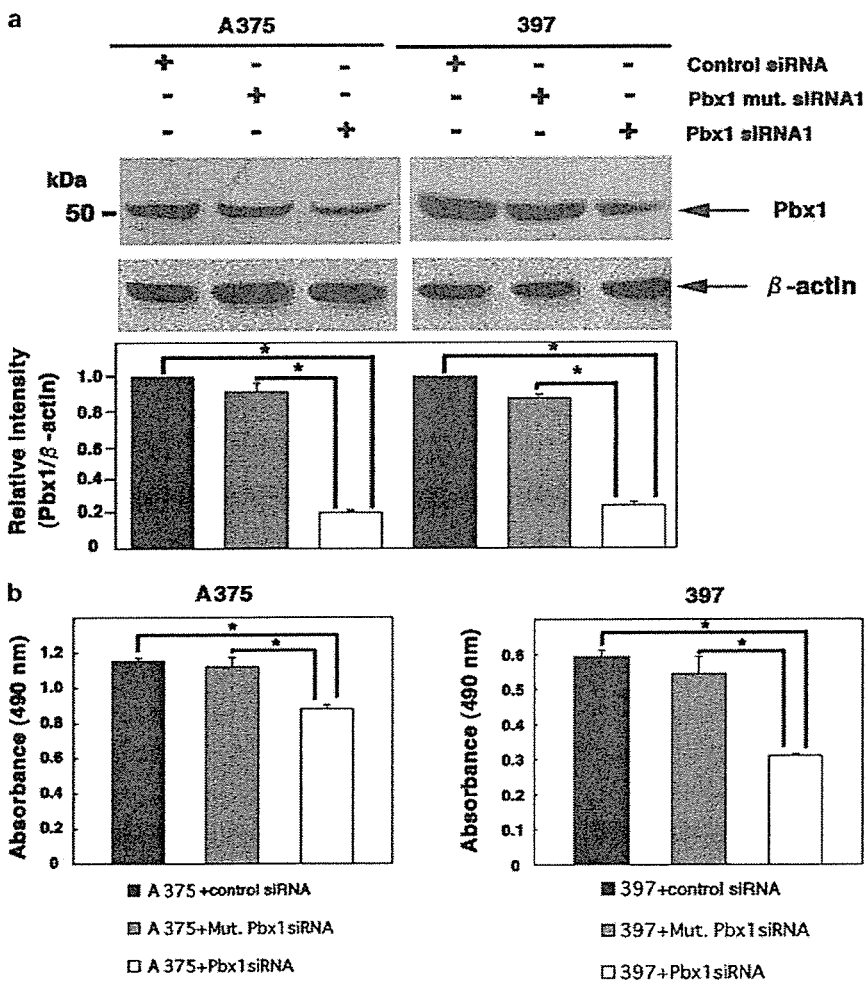

Figure 4 Melanoma cell growth is suppressed by Pbx1 siRNAs. (a) Upper panel: Western blot analysis of Pbx1 in control siRNA-, mutated-Pbx1 siRNA- and Pbx1 siRNA-transduced melanoma cells. Lower panel: Relative intensity of Pbx1 protein expression calculated as the ratio of Pbx1 vs β-actin. $*P<0.05$. (b) Cell proliferation of melanoma cells transfected with each siRNA. $*P<0.05$. Each experiment was performed in triplicate.

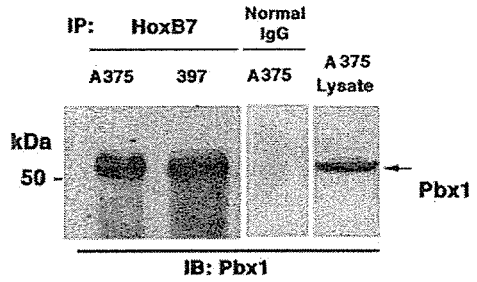

Figure 5 Pbx1 binds HoxB7. Interaction between Pbx1 and HoxB7 as assessed by immunoprecipitation. A375 and 397 cell lysates were immunoprecipitated with anti-HoxB7 antibody and immunoblotted with anti-Pbx1 antibody. Sodium dodecyl sulfate–polyacrylamide gel electrophoresis was carried out under the non-reducing condition.

of Pbx1 with the siRNAs slightly reduced the mRNA expression of HoxB7 (Figure 6a). It remains uncertain whether Pbx1 binds directly to the promoter region of the HoxB7 gene. HoxB7 is reported to regulate the expression of basic fibroblast growth factor (bFGF), angiopoietin-2 (Ang-2), matrix metalloprotease 9 (MMP9), growth-related oncogene-α (GROα), interleukin-8 (IL-8) and vascular endothelial growth factor (VEGF) (Care *et al.*, 1996, 2001). We thus evaluated the effects of Pbx1 knockdown on the expression of the target genes. As shown in Figure 6b, knockdown of Pbx1 markedly reduced the level of bFGF mRNA, and mildly did those of Ang-2 and MMP mRNAs, whereas those of GROα, IL-8 and VEGF were unchanged. Pbx1 knockdown significantly reduced protein levels of Ang-2 and MMP9, but it did not seem to have any effect on the protein levels of bFGF. This may be owing to the short culture duration and/or long half-life of bFGF protein. We obtained similar results in 397 cells (data not shown).

We further examined whether enforced expression of PLZF in melanoma cells would reduce HoxB7, bFGF, Ang-2 and MMP9. Quantitative RT–PCR analysis revealed that transcripts of all of these were significantly reduced in both A375P and 397P cells (Figure 7). These data suggest that the PLZF–Pbx1 axis is important in regulating HoxB7 target genes via Pbx1/HoxB7 heterocomplex formation.

Discussion

In this study, we performed DNA microarray analysis and found that Pbx1 is a prominent transcription factor targeted by PLZF. Pbx1 was highly expressed in the A375 and 397 cell lines, and its expression was markedly reduced by the expression of PLZF. Moreover, we showed that the growth suppression caused by ectopic expression of PLZF is reversed by enforced expression of Pbx1. Knockdown of Pbx1 using siRNAs in A375 and 397 cells reduced its protein levels by approximately 80%. Pbx1 siRNAs significantly inhibited cell growth in culture, thus suggesting that Pbx1 is a downstream target of PLZF in melanoma cell growth regulation.

In order to determine whether PLZF suppresses Pbx1 gene expression directly or indirectly, we examined the ability of PLZF to repress the Pbx1 promoter. We found that the 3.0 kb upstream region of the Pbx1 gene (nucleotides −3.0 kb to 0) contains seven possible PLZF DNA-binding consensus sequences. We then performed reporter assay and EMSA to examine the direct binding of PLZF in the Pbx1 promoter region. EMSA suggested the presence of an interactive site (Site 1) for PLZF in the 3.0-kb of upstream Pbx1 gene sequences. Deletion of Site 1, however, did not recover Pbx1 gene expression. These data suggest multiple direct and/or indirect regulation mechanisms for Pbx1 gene expression by PLZF. Further analysis is required for elucidating these mechanisms.

Pbx1 was originally identified at t(1;19) chromosomal translocations in acute pre-B-cell leukemias (Kamps *et al.*, 1990; Nourse *et al.*, 1990), and it has also been described as a transcriptional activator. Pbx1 is known to interact with a number of Hox proteins through the YPWM motif located at the N-termini of the homeodomains in Hox proteins and to regulate the function of Hox proteins (Chang *et al.*, 1995; Shanmugam *et al.*, 1997). It has been reported that Pbx1 cooperates in the cellular proliferation and transformation induced by Hox proteins (Krosl *et al.*, 1998). Krosl *et al.* (1998) showed that the ability of HoxB4 and HoxB3 to interact with Pbx1 is critical for transformation of Rat-1 cells, that Hox proteins have a notable effect on cell growth, and that Pbx1 further enhances this effect. Although HoxB7 is reportedly involved in melanoma growth (Care *et al.*, 1996, 2001; Felicetti *et al.*, 2004), there have been few reports on the relationship between Pbx1 and the progression of melanoma. We showed here that immunoprecipitation of HoxB7 from A375 and 397 melanoma cell lines co-precipitated a 52-kDa protein that was recognized by an anti-Pbx1 antibody, thus suggesting that Pbx1 physically interacts with HoxB7. Our data indicate that Pbx1 plays an important role in melanoma growth and that it forms heterocomplexes with HoxB7, which suggests that molecular events mediated by the Pbx1–HoxB7 heterocomplex are altered in melanoma cells when Pbx1 is suppressed by PLZF.

Previous studies have identified some HoxB7 target genes. bFGF was identified as the main target of HoxB7 in melanoma cell lines (Care *et al.*, 1996). In addition, VEGF, GROα, IL-8, Ang-2 and MMP9 were found to be upregulated in HoxB7-transduced cells (Care *et al.*, 2001). Based on these reports, we analysed the effect of Pbx1 knockdown on HoxB7 target genes. We found that knockdown of Pbx1 slightly downregulated HoxB7 itself and substantially downregulated bFGF, Ang-2 and MMP9, but not VEGF, GROα or IL-8. This suggests that HoxB7 target genes are differentially regulated by HoxB7–Pbx1 or by another HoxB7 complex. Interestingly, these factors are strongly associated with tumor angiogenesis and invasion (Becker *et al.*, 1989; Ahmad *et al.*, 2001; Etoh *et al.*, 2001; Johnson *et al.*, 2004). The Pbx1–HoxB7 complex may

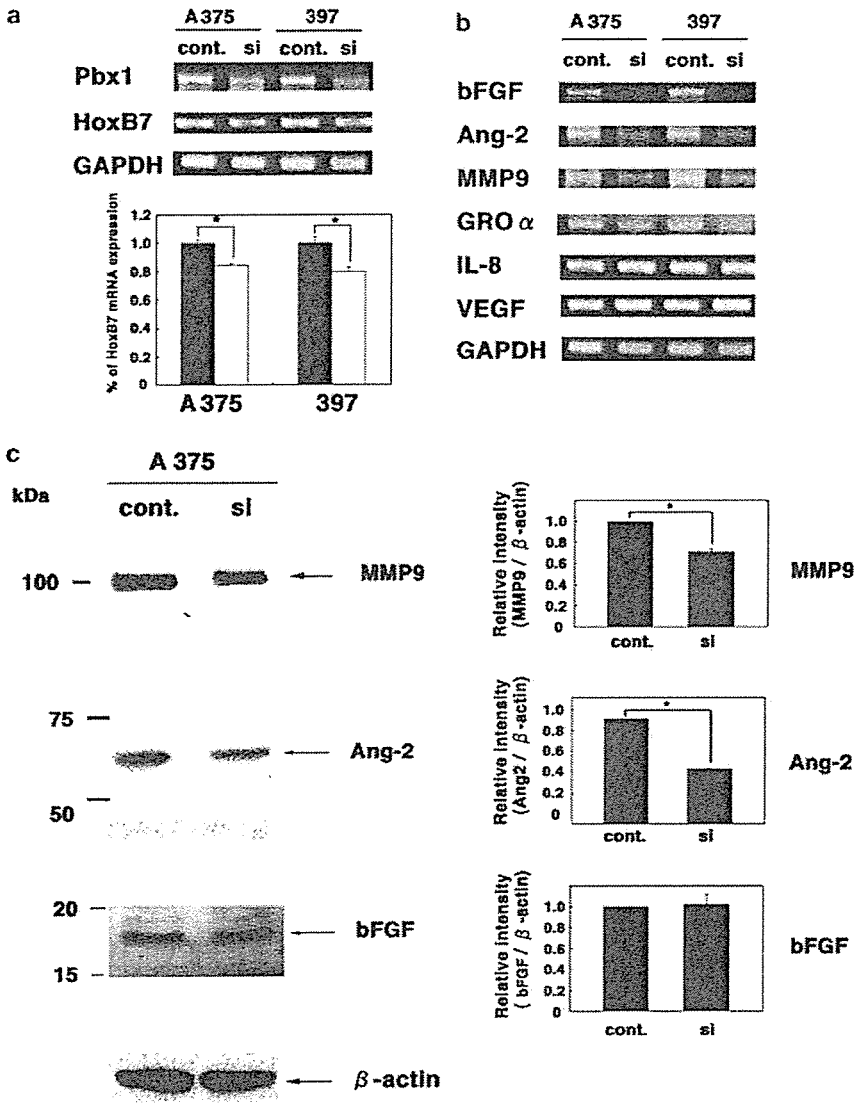

Figure 6 Expression of HoxB7 and its target genes is modulated by knockdown of Pbx1. (**a**) Upper panel: RT–PCR analysis of HoxB7 expression in Pbx1-knockdown melanoma cells and control cells. Lower panel: Relative intensity of Pbx1 and HoxB7 mRNA expression in Pbx1-knockdown melanoma cells and control cells, which was calculated as a ratio vs the expression of GAPDH. $^*P<0.05$. (**b**) RT–PCR analysis of HoxB7 target gene expression in each cell type. (**c**) Immunoblot analysis of Ang-2, MMP9 and bFGF in Pbx1-knockdown melanoma cells and control cells. Relative intensity of each protein was calculated as a ratio vs the expression of β-actin. $^*P<0.05$.

thus play a very important role in melanoma growth, and its suppression could be a major cause of the reduction in PLZF-mediated growth in melanoma. This is supported by previous reports that PLZF is expressed in melanocytes but not in melanoma cells, and that the pattern of PLZF expression inversely correlates with that of HoxB7 (Care *et al*., 1996, 1998).

In this study, we showed that the suppression of Pbx1 expression by PLZF downregulates some HoxB7 target genes, including bFGF, Ang-2 and MMP9. The data indicated that the changes in the molecular network caused by the loss of PLZF may play an important role in the progression of melanoma. Further analyses of the PLZF–Pbx1 network will assist in the discovery of target molecules for the development of novel anti-melanoma drugs.

Materials and methods

Materials

Human melanoma cell lines A375 and 397 were generously provided by Dr Kawakami (Keio University, Tokyo, Japan) (Sumimoto *et al*., 2004). Cells were grown in Roswell Park Memorial Institute medium 1640 supplemented with 10% fetal calf serum (FCS), penicillin (100 U/ml) and streptomycin

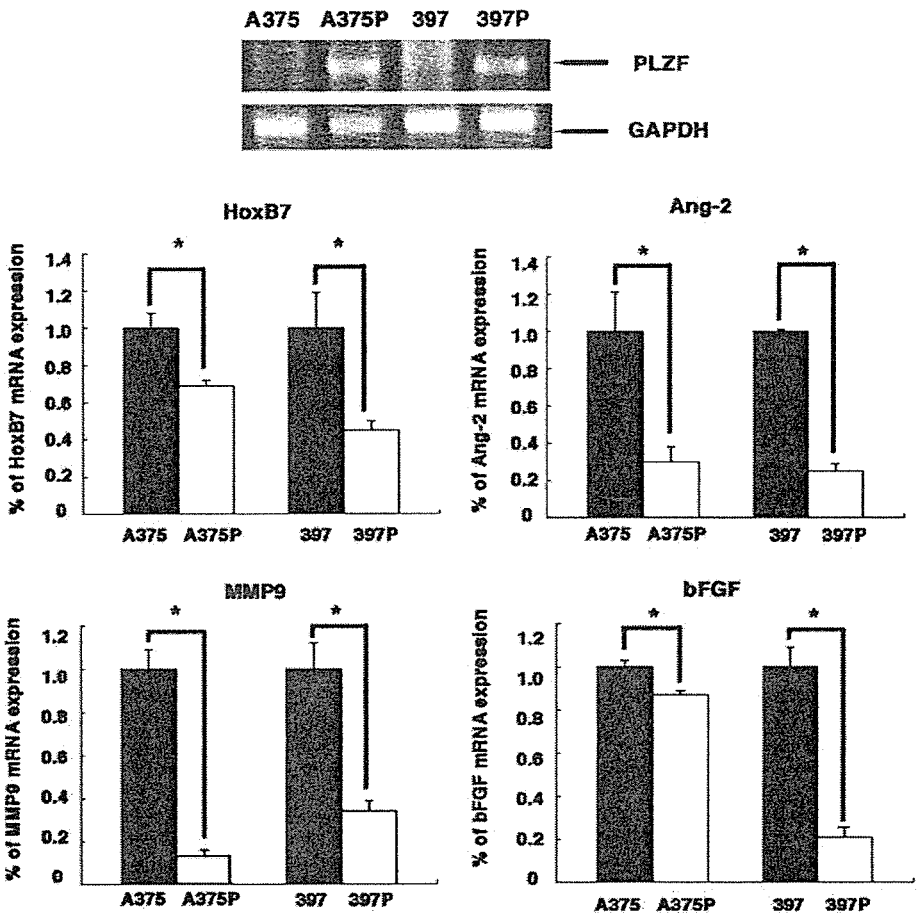

Figure 7 Expression of HoxB7, bFGF, Ang-2 and MMP9 is suppressed by the transduction of PLZF in melanoma cells. Upper panel: RT–PCR analysis for PLZF mRNA in A375, A375P, 397 and 397P cells. GAPDH, glyceraldehyde 3-phosphate dehydrogenase. PLZF was evaluated at 35 cycles, whereas control GAPDH evaluated at 24 cycles. Lower panel: qRT–PCR for HoxB7, bFGF, Ang-2 and MMP9 mRNA in PLZF-expressing melanoma cells and parental cells. $^*P<0.05$.

sulfate (100 μg/ml) at 37°C in an atmosphere containing 5% CO_2. Antibodies used were as follows: rabbit anti-Pbx1 polyclonal antibody (Santa Cruz Biotechnology, Santa Cruz, CA, USA), mouse anti-PLZF monoclonal antibody (Oncogene Research Products, San Diego, CA, USA), rabbit anti-HoxB7 polyclonal antibody (CeMines, Golden, CO, USA), rabbit anti-bFGF polyclonal antibody (Abcam, Cambridge, UK), mouse anti-Ang-2 monoclonal antibody, goat anti-MMP9 monoclonal antibody (R&D, Tokyo, Japan), goat horseradish peroxidase-conjugated anti-rabbit antibody, donkey horseradish peroxidase-conjugated anti-goat antibody and goat horseradish peroxidase-conjugated anti-mouse antibody (Promega, Madison, WI, USA).

Plasmid and adenovirus vector construction

A plasmid encoding PLZF was generated by subcloning the human PLZF cDNA into pcDNA3.1/Hygro. (Invitrogen, Carlsbad, CA, USA). A plasmid encoding Pbx1 was generated by subcloning Pbx1 cDNA into pME18S (Tanaka *et al.*, 2004). The Pbx1 promoter 3.0 kb was subcloned into pGL3 (Promega). Transfection of plasmids was performed with LipofectAMINE (Invitrogen) according to the manufacturer's instructions. To assess transfection efficiency of pME18S-Pbx1 in 375P cells, both PME18S-Pbx1 and pME18S-ECFP plasmids were transfected into 375P cells and CFP-positive cells were counted. Adenovirus vector (Ax) carrying PLZF was prepared using an adenovirus expression vector kit (Takara Biomedicals, Kyoto, Japan). PLZF was subcloned into the cosmid cassette pAxCAw. Ax containing the CA promoter and PLZF (AxPLZF) was generated by the COS-TPC method according to the manufacturer's protocol. A375 and 397 cells were infected with Axs at an MOI of 50–200 for 1 h. Ax expressing LacZ (Ax-LacZ) and GFP (Ax-GFP) were used as controls to exclude the effects of Ax itself.

RT–PCR and quantitative real-time PCR

Primer sequences for RT–PCR are listed in Table 2. Total RNA was isolated from cultured melanoma cells using Trizol Reagent (Invitrogen), and was treated with DNase I (Clontech, Palo Alto, CA, USA) at 37°C for 30 min to remove contaminating genomic DNA. RT–PCR was performed using RT–PCR High Plus (Toyobo, Osaka, Japan) according to the manufacturer's instructions. cDNA was reverse transcribed from total RNA for 30 min at 60°C, and heated to 94°C for 2 min. Amplification was performed using a GeneAmp PCR System 9700 (Applied Biosystems, Foster City, CA, USA) for

Table 2 Primer sequences used in this study

Gene	*Upper primer (5′–3′)*	*Lower primer (5′–3′)*
Pbx1	GGAGATTGAGCGGATGGT	CATGGGCTGACACATTGGTAG
HoxB7	AAGGAGCAGAGGGACTCGGACT	AAATCTTGATCTGTCTTTCCGTGAG
bFGF	CCCAAGCGGCTGTAC	ATACTGCCCAGTTCGTTTCA
Ang-2	GCAGCCTATAACAACTTTCGGAAGA	TATTTCTATCATCACAGCCGTCT
MMP9	GAGATGCGTGGAGAGTCGAAA	CAAAGGCGTCGTCAATCA
GROα	ACTGCTGCTCCTGCTCCTGGTAGCC	TTTCCGCCCATTCTTGAGTGT
IL-8	GAATCTAAATTATCAGTCATA	CAGTGAACATTATAGATCTAT
VEGF	CTGCTGTCTTGGGTGCATTG	TCACCGCCTCGGCTTGTCACA
GAPDH	CGTATTGGGCGCCTGGTCACCAG	TCGCTCCTGGAAGATGGTGATGGG

Abbreviations: Ang-2, angiopoietin-2; bFGF, basic fibroblast growth factor; GAPDH, glyceraldehyde-3-phosphate dehydrogenase; GROα, growth-related oncogene-α; IL-8, interleukin-8; MMP9, matrix metalloprotease 9; Pbx1, pre-B-cell leukemia transcription factor 1; VEGF, vascular endothelial growth factor.

24 or 35 cycles. The cycle profile consisted of 1 min at 94°C for denaturation and 1.5 min at 60°C for annealing and primer extension. To evaluate amplification, 5 μl of the reaction mixture was electrophoresed on a 1.0% agarose gel containing ethidium bromide. We performed at least three independent studies and confirmed similar results. Quantitative real-time PCR (qRT–PCR) was performed using the ABI PRISM 7700 sequencer detection system (Perkin–Elmer Applied Biosystems, Foster City, CA, USA). Primers and probe were purchased from Applied Biosystems (Assays-on-Demand). RT–PCR mixtures were prepared according to the manufacturer's instructions for the TaqMan One-Step RT–PCR Master Mix Reagent kit (Perkin–Elmer Applied Biosystems). Probe was labeled with a reporter fluorescent dye (6-carboxyfluorescein) at the 5′ end. For glyceraldehyde 3-phosphate dehydrogenase (GAPDH) detection, Pre-Developed TaqMan Assay Reagent (Perkin–Elmer Applied Biosystems) was added. The thermal conditions were 48°C for 30 min for RT and 95°C for 10 min, followed by 45 amplification cycles of 95°C for 15 s for denaturing and 60°C for 1 min for annealing and extension. PCR products were sequenced to confirm proper amplification. To compare mRNA expression, results were determined as relative values against GAPDH as an internal reference. There were $n=3$ samples in each group.

siRNA experiments

siRNA sequences used in this study were as follows: Pbx1 siRNA sequences were 5′-CCGCAGGGCATCAGTGCTA-3′ (siRNA1) and 5′-CGACAGAAATCCTGAATGA-3′ (siRNA2), and the mutated Pbx1 siRNA sequences were 5′-CC ACAAGGCATTAGCGCTA-3′ (mut. siRNA1) and 5′-CG ACCGAGATCCTAAACGA-3′ (mut. siRNA2) (B-Bridge International, Sunnyvale, CA, USA). Scrambled siRNA directed against 5′-GCGCGCTTTGTAGGATTCG-3′ was also used as a negative control. This sequence was not present in any mammalian mRNAs in the National Center for Biotechnology Information database. siRNA transfection was performed with CodeBreaker siRNA Transfection Reagent (Promega). Briefly, cells (5×10^5) were incubated in 35-mm plates with siRNA (final concentration, 40 nM)–CodeBreaker Reagent (15 μl) mixture in serum-free medium for 24 h. Cells were then grown in media with 10% FCS.

Microarray analysis

Total RNA was isolated from LacZ or PLZF Ax-infected melanoma cells at 48 h post-infection. The Acegene Human oligo chip 30K (Hitachi Software Engineering, Yokohama, Japan) containing 30 000 genes was used to compare gene expression in melanoma cells infected with PLZF or LacZ adenovirus. Arrays were screened according to the manufacturer's protocol. Fluorescent images of hybridized microarrays were obtained with a CRBIO IIe microarray scanner (Hitachi Software Engineering), and images were analysed with DNAsis Array software (Hitachi Software Engineering).

EMSA

Nuclear protein extracts were prepared using celLytic NuCLEAR Extraction Kit (Sigma, St Louis, MO, USA). Biotin-labeled oligomers containing PLZF-binding sequences (Sites 1, 2, 3, 4, 5, 6 and 7) were bound to nuclear extracts. Binding reactions were performed using the LightShift EMSA Optimization and Control kit (Pierce, Rockford, IL, USA) according to the manufacturer's instructions. Reaction mixtures were incubated on ice for 60 min. Biotin-unlabeled oligomers were used as competitors, and when present, were added to the mixtures 30 min before the other reagents. Binding reactions were subjected to EMSA on 4% nondenaturing polyacrylamide gels in 0.5 × Tris-Borate-EDTA buffer, and detection was performed using a LightShift Chemiluminescent EMSA Kit (Pierce) according to the manufacturer's instructions. Sequences of the probes used in this study were as follows: Site 1, 5′-CCTCCAGATCCAGTT CATCC-3′; Site 2, 5′-CGGGGTAAGACAGTTGCAAT-3′; Site 3, 5′-TTTGAGTATATAGTTTTGTG-3′; Site 4, 5′-TTTAAAAAAAACAGTTTAAAA-3′; Site 5, 5′-ACTGTG TACACAGTCAGATT-3′; Site 6 5′-AAAAATGACACA GTTTGGTA-3′; Site 7, 5′-GCTGGAACTACAGTAC CATT-3′ and mutated-Site 1, 5′-CCTCCAGAGAAAGTT CATCC-3′.

Luciferase reporter assays

Melanoma cells were cultured in 24-well plates and grown to 70% confluence. Cells were transfected with 0.8 μg/well of pGL3-Pbx1 plasmid DNA using LipofectAMINE (Invitrogen). Transfected cells were harvested at 24 h post-transfection, and lysates were assayed for luciferase activity with a Dual-Glo Luciferase Assay System (Promega) according to the manufacturer's protocol.

Immunoprecipitation and Western blotting

A375 and 397 cells were transiently transfected with pME18S-Pbx1 plasmid. Cells were lysed 48 h after transfection and equivalent amounts of lysate protein were subjected into immunoprecipitation. Immunoprecipitation and Western blotting were performed as described previously (Goishi *et al.*,

1995). After membranes were washed three times at intervals of 10 min with 0.05% Tween-20 in phosphate-buffered saline, horseradish peroxidase conjugate was detected by chemiluminescence with an ECL kit (Amersham, Buckinghamshire, UK) and autofluorography.

Acknowledgements

We thank Drs T Tsuda, T Jyokou, E Tan, M Tohyama, H Iwabuki, T Kikugawa, Y Kinugasa and E Koya for technical assistance, helpful comments and discussion.

References

Ahmad SA, Liu W, Jung YD, Fan F, Wilson M, Reinmuth N *et al.* (2001). The effects of angiopoietin-1 and -2 on tumor growth and angiogenesis in human colon cancer. *Cancer Res* **61**: 1255–1259.

Barna M, Hawe N, Niswander L, Pandolfi PP. (2000). Plzf regulates limb and axial skeletal patterning. *Nat Genet* **25**: 166–172.

Barna M, Merghoub T, Costoya JA, Ruggero D, Branford M, Bergia A *et al.* (2002). Plzf mediates transcriptional repression of HoxD gene expression through chromatin remodeling. *Dev cell* **3**: 499–510.

Becker D, Meier CB, Herlyn M. (1989). Proliferation of human malignant melanomas is inhibited by antisense oligodeoxynucleotides targeted against basic fibroblast growth factor. *EMBO J* **8**: 3685–3691.

Care A, Silvani A, Meccia E, Mattia G, Stoppacciaro A, Parmiani G *et al.* (1996). HOXB7 constitutively activates basic fibroblast growth factor in melanomas. *Mol Cell Biol* **16**: 4842–4851.

Care A, Silvani A, Meccia E, Mattia G, Peschle C, Colombo MP. (1998). Transduction of the SkBr3 breast carcinoma cell line with the HOXB7 gene induces bFGF expression, increases cell proliferation and reduces growth factor dependence. *Oncogene* **16**: 3285–3289.

Care A, Felicetti F, Meccia E, Bottero L, Parenza M, Stoppacciaro A *et al.* (2001). HOXB7: a key factor for tumor-associated angiogenic switch. *Cancer Res* **61**: 6532–6539.

Chang CP, Shen WF, Rozenfeld S, Lawrence HJ, Largman C, Cleary ML. (1995). Pbx proteins display hexapeptide-dependent cooperative DNA binding with a subset of Hox proteins. *Genes Dev* **9**: 663–674.

Chen Z, Brand NJ, Chen A, Chen SJ, Tong JH, Wang ZY *et al.* (1993). Fusion between a novel Kruppel-like zinc finger gene and the retinoic acid receptor-alpha locus due to a variant t(11;17) translocation associated with acute promyelocytic leukaemia. *EMBO J* **12**: 1161–1167.

Costoya JA, Hobbs RM, Barna M, Cattoretti G, Manova K, Sukhwani M *et al.* (2004). Essential role of Plzf in maintenance of spermatogonial stem cells. *Nat Genet* **36**: 653–659.

Etoh T, Inoue H, Tanaka S, Barnard GF, Kitano S, Mori M. (2001). Angiopoietin-2 is related to tumor angiogenesis in gastric carcinoma: possible *in vivo* regulation via induction of proteases. *Cancer Res* **61**: 2145–2153.

Felicetti F, Bottero L, Felli N, Mattia G, Labbaye C, Alvino E *et al.* (2004). Role of PLZF in melanoma progression. *Oncogene* **23**: 4567–4576.

Goishi K, Higashiyama S, Klagsbrun M, Nakano N, Umata T, Ishikawa M *et al.* (1995). Phorbol ester induces the rapid processing of cell surface heparin-binding EGF-like growth factor: conversion from juxtacrine to paracrine growth factor activity. *Mol Biol Cell* **6**: 967–980.

Heinemeyer T, Wingender E, Reuter I, Hermjakob H, Kel AE, Kel OV *et al.* (1998). Databases on transcriptional regulation: TRANSFAC, TRRD and COMPEL. *Nucleic Acids Res* **26**: 364–370.

Hong SH, David G, Wong CW, Dejean A, Privalsky ML. (1997). SMRT corepressor interacts with PLZF and with the PML-retinoic acid receptor alpha (RARalpha) and PLZF-RARalpha oncoproteins associated with acute promyelocytic leukemia. *Proc Natl Acad Sci USA* **94**: 9028–9033.

Johnson C, Sung HJ, Lessner SM, Fini ME, Galis ZS. (2004). Matrix metalloproteinase-9 is required for adequate angiogenic revascularization of ischemic tissues: potential role in capillary branching. *Circ Res* **94**: 262–268.

Kamps MP, Murre C, Sun XH, Baltimore D. (1990). A new homeobox gene contributes the DNA binding domain of the t(1;19) translocation protein in pre-B ALL. *Cell* **60**: 547–555.

Krosl J, Baban S, Krosl G, Rozenfeld S, Largman C, Sauvageau G. (1998). Cellular proliferation and transformation induced by HOXB4 and HOXB3 proteins involves cooperation with PBX1. *Oncogene* **16**: 3403–3412.

Li JY, English MA, Ball HJ, Yeyati PL, Waxman S, Licht JD. (1997). Sequence-specific DNA binding and transcriptional regulation by the promyelocytic leukemia zinc finger protein. *J Biol Chem* **272**: 22447–22455.

Mann RS, Chan SK. (1996). Extra specificity from extradenticle: the partnership between HOX and PBX/EXD homeodomain proteins. *Trends Genet* **12**: 258–262.

McConnell MJ, Chevallier N, Berkofsky-Fessler W, Giltnane JM, Malani RB, Staudt LM *et al.* (2003). Growth suppression by acute promyelocytic leukemia-associated protein PLZF is mediated by repression of c-*myc* expression. *Mol Cell Biol* **23**: 9375–9388.

Nourse J, Mellentin JD, Galili N, Wilkinson J, Stanbridge E, Smith SD *et al.* (1990). Chromosomal translocation t(1;19) results in synthesis of a homeobox fusion mRNA that codes for a potential chimeric transcription factor. *Cell* **60**: 535–546.

Shanmugam K, Featherstone MS, Saragovi HU. (1997). Residues flanking the HOX YPWM motif contribute to cooperative interactions with PBX. *J Biol Chem* **272**: 19081–19087.

Sumimoto H, Miyagishi M, Miyoshi H, Yamagata S, Shimizu A, Taira K *et al.* (2004). Inhibition of growth and invasive ability of melanoma by inactivation of mutated BRAF with lentivirus-mediated RNA interference. *Oncogene* **23**: 6031–6039.

Tanaka M, Nanba D, Mori S, Shiba F, Ishiguro H, Yoshino K *et al.* (2004). ADAM binding protein Eve-1 is required for ectodomain shedding of epidermal growth factor receptor ligands. *J Biol Chem* **279**: 41950–41959.

Wong CW, Privalsky ML. (1998). Components of the SMRT corepressor complex exhibit distinctive interactions with the POZ domain oncoproteins PLZF, PLZF-RARalpha, and BCL-6. *J Biol Chem* **273**: 27695–27702.

Yeyati PL, Shaknovich R, Boterashvili S, Li J, Ball HJ, Waxman S *et al.* (1999). Leukemia translocation protein PLZF inhibits cell growth and expression of cyclin A. *Oncogene* **18**: 925–934.

Journal of Dermatological Science (2007) 45, 69–72

ELSEVIER

Dermatological SCIENCE

www.intl.elsevierhealth.com/journals/jods

LETTER TO THE EDITOR

Epiregulin, a member of the EGF family, is over-expressed in psoriatic epidermis

KEYWORDS
Epiregulin; EGF family; Psoriasis; TGF-α; Amphiregulin; Northern blot; *In situ* hybridization

Psoriasis is characterized by the hyperproliferation of keratinocytes, altered epidermal differentiation, dermal angiogenesis, and a dense lesional infiltrate in the dermal and epidermal component, consisting mainly of macrophages, lymphocytes, and neutrophils. To date, the expression of many regulatory molecules has been well clarified in psoriatic epidermis. Previous reports have shown that various cytokines and growth factors are over-expressed in psoriatic epidermis [1]. Keratinocytes are the main component cells of the epidermis, and their growth is regulated by both positive and negative mediators [2]. Of these mediators, the most important mechanism for the proliferation of keratinocytes is the signal from the epidermal growth factor (EGF) receptor. The EGF family consists of EGF, transforming growth factor-α (TGF-α), heparin binding EGF-like growth factor (HB-EGF), amphiregulin, epiregulin, betacellulin, epigen, neuregulin (NRG)-1, NRG-2, NRG-3, and NRG-4, and the EGF receptor (EGFR) family consists of EGFR (also called ErbB1), ErbB2, ErbB3, and ErbB4 [2]. Previous reports have shown that TGF-α, amphiregulin and HB-EGF are over-expressed in psoriatic epidermis [3–5]. Given that epiregulin is a member of the EGF family and an autocrine growth factor for normal human keratinocytes [6], we speculated that epiregulin is over-expressed in psoriasis. To prove our hypothesis, we investigated the expression of epiregulin as well as TGF-α and amphiregulin in psoriatic epidermis.

All procedures that involved human subjects received prior approval from the Ethics Committee of Ehime University School of Medicine, Toon, Ehime, Japan, and all subjects provided written informed consent. Twelve psoriatic lesional skin samples and 10 normal healthy skin samples were obtained. To exclude the RNA from the dermis, we separated the epidermis from the dermis by a heat-separation technique. The specimens were heated at 60 °C in sterile saline for 1 min. The epidermis was then separated from the dermis, immediately frozen in liquid nitrogen. We confirmed that heat-separation did not influence on the results. Total RNA was extracted from snap-frozen epidermis by using Isogen (Nippon Gene, Tokyo, Japan). Northern blot analysis was performed as previously described [6]. TGF-α mRNA was detected in all the psoriatic

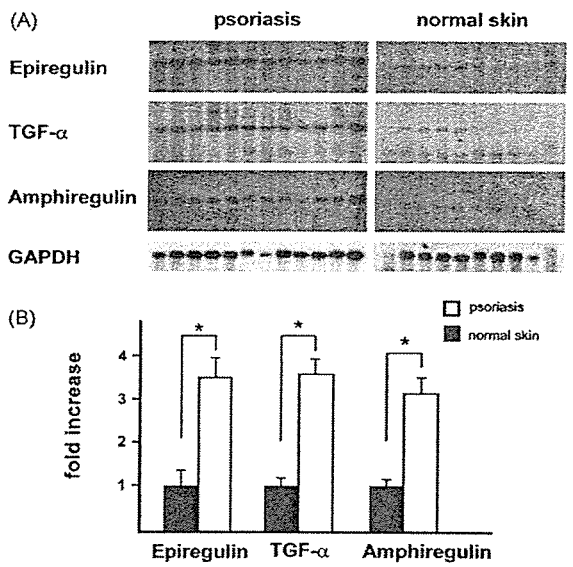

Fig. 1 mRNA expression of epiregulin, TGF-α, and amphiregulin in psoriatic epidermis. (A) The mRNA expression levels of epiregulin, TGF-α, and amphiregulin were analyzed by Northern blotting in psoriatic and normal epidermis. (B) Densitometric analysis of Northern blotting. Quantification of the signals was performed by using a densitometer and analyzed by ImageQuant software. Normal epidermis signal values were taken as 100% control. The signals were adjusted by GAPDH as an internal standard. $^{*}p < 0.05$.

doi:10.1016/j.jdermsci.2006.08.010

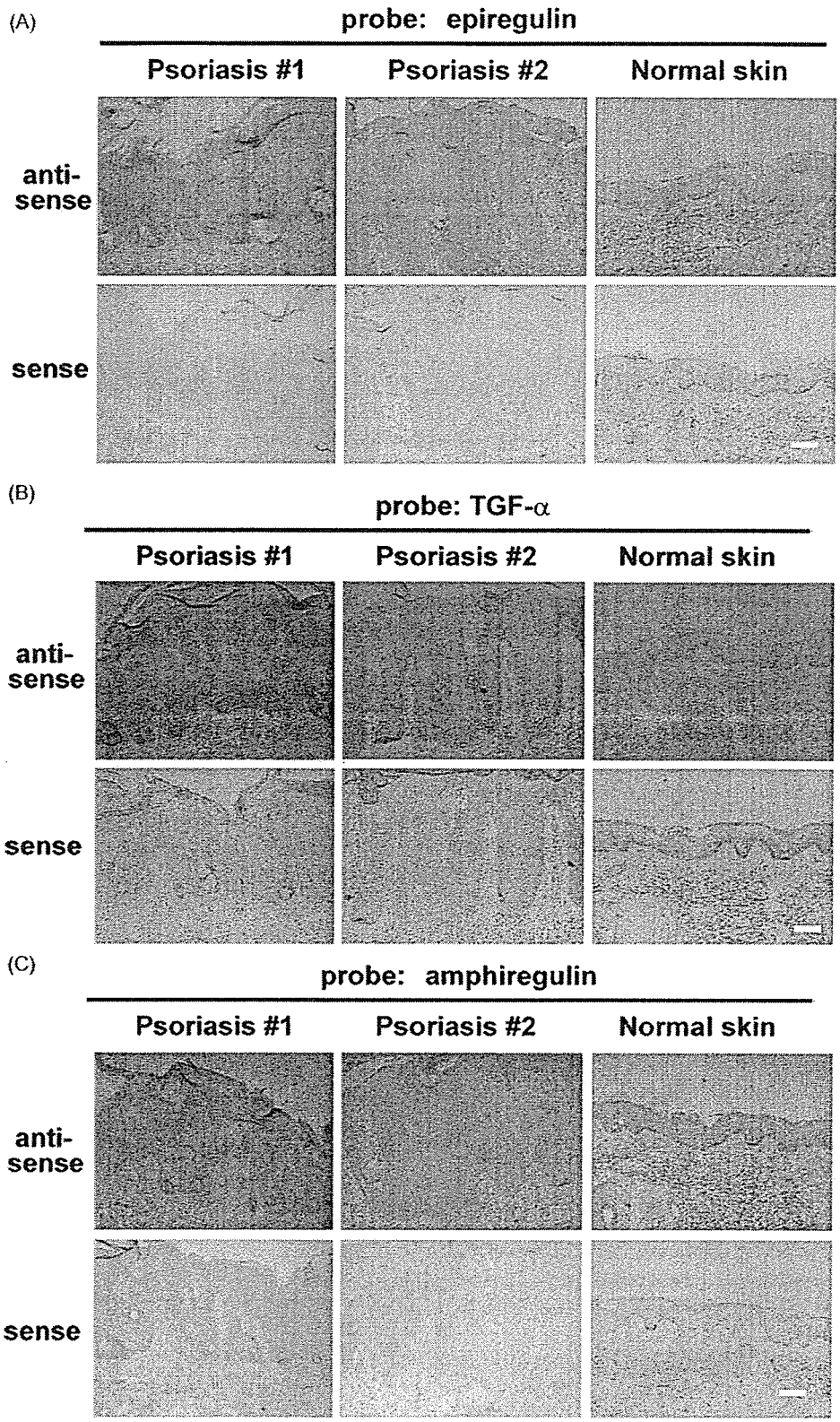

Fig. 2 *In situ* hybridization of epiregulin, TGF-α, and amphiregulin in psoriatic epidermis. *In situ* hybridization was performed using an automated *in situ* hybridization protocol. (A) Epiregulin; (B) TGF-α; (C) amphiregulin. Bar: 100 μm.

epidermis samples and was expressed at higher levels than in the normal epidermis. Amphiregulin mRNA was also detected in all the psoriatic epidermis samples and was expressed at higher levels than in the normal epidermis. The 4.8-kb transcript of epiregulin was detected in both normal and psoriatic epidermis, although the expression level was higher in the psoriatic epidermis than in the normal epidermis (Fig. 1A). Densitometric analysis revealed that TGF-α and amphiregulin mRNA were elevated by 3.6- and 3.2-fold, respectively. Epiregulin mRNA was also increased in psoriatic epidermis by 3.5-fold (Fig. 1B). To identify the localization of epiregulin, TGF-α, and amphiregulin mRNA, we performed *in situ* hybridization as previously described [7]. In normal skin, we found that epiregulin mRNA was expressed in the basal layer and that its expression was very faint. However, epiregulin mRNA was over-expressed in the spinous layer, mainly in the uppermost region of the spinous layer, but not in the basal layer of the psoriatic lesional epidermis (Fig. 2A). TGF-α and amphiregulin mRNA were also over-expressed in the spinous layer, but not in the basal layer, of the psoriatic lesional epidermis (Fig. 2B and C).

Considerable evidence currently exists to support the concept that psoriasis is mediated by many inflammatory cytokines. There is a predominance of Th1 cytokines, mainly interferon gamma (IFN-γ), in contrast to the predominance of Th2 cytokines found in atopic dermatitis. This immune-mediated aspect of psoriasis pathogenesis has been confirmed by the use of cyclosporine or targeted therapies against T cells, CD11a, or TNF-α [1]. With regard to keratinocytes, psoriatic plaques represent a hyperproliferative condition and deregulated differentiation [1]. Keratinocytes are the main component cells of the epidermis, and the important mechanism for keratinocyte growth is the EGF receptor-ligand system. In this EGF receptor-ligand system, the signal from ErbB1 (EGFR) is important for keratinocyte growth. TGF-α, HB-EGF, amphiregulin and epiregulin are autocrine growth factors and all bind to ErbB1 [2]. Previous reports have shown that TGF-α and amphiregulin mRNA are over-expressed in psoriatic lesional skin and play important roles for the keratinocyte proliferation of psoriatic epidermis, suggesting that all members of the EGF family are up-regulated in psoriatic epidermis [3–5]. In this study, we investigated the mRNA expression of epiregulin as well as TGF-α and amphiregulin in psoriatic and normal epidermis. The mRNA expression of TGF-α and amphiregulin was elevated in psoriatic epidermis, as compared to normal skin, as previously reported. The mRNA expression of epiregulin was also increased in psoriatic epidermis. Over-expressed epiregulin mRNA was localized in the spinous layer, but not in the basal layer, of the psoriatic epidermis. TGF-α and amphiregulin mRNA localization in psoriatic epidermis is within the spinous layer. This deregulated growth factor signaling may contribute to the hyperproliferative condition of psoriasis. In fact, a transgenic mouse with the amphiregulin gene revealed a psoriasis-like phenotype [8]. Based on our results and previous reports, a cross-induction mechanism of the keratinocyte-derived EGF family is involved in the development of psoriatic hyperproliferative epidermis.

Intracellular signaling systems such as Erk/JNK or MAP kinase, which are activated by the EGF family, are up-regulated in psoriatic epidermis [9]. Recent studies have shown that transgenic mice over-expressing a constitutive active form of STAT3 develop a psoriasis-like phenotype [10]. Because these molecules are downstream of EGFR signaling, an over-expressed EGF family may contribute to the pathogenesis of psoriasis by activating signal transduction molecules. Because topical treatment will probably remain the mainstay of psoriasis therapy for most patients, and aberrant expression of epiregulin as well as TGF-α and amphiregulin could facilitate the development of proliferative pathological conditions of psoriasis, additional targeting of such signal transduction molecule and/or growth factors may enhance anti-psoriatic therapy.

In conclusion, we have demonstrated the over-expression of epiregulin in psoriatic epidermis. Autocrine EGF-related growth factors may play an important role in the pathogenesis of psoriasis.

Acknowledgments

This work was partly supported by Health Sciences Research Grants for Research on Specific Diseases from the Ministry of Health, Labor, and Welfare of Japan and a Grant-in-Aid for Scientific Research from the Ministry of Education, Culture, Sports, Science, and Technology of Japan. We would also like to thank Teruko Tsuda and Eriko Tan for their technical assistance.

References

[1] Schon MP, Boehncke WH. Psoriasis. N Engl J Med 2005;352:1899–912.
[2] Hashimoto K. Regulation of keratinocyte function by growth factors. J Dermatol Sci 2000;24:S46–50.
[3] Cook PW, Pittelkow MR, Keeble WW, Graves-Deal R, Coffey Jr RJ, Shipley GD. Amphiregulin messenger RNA is elevated

in psoriatic epidermis and gastrointestinal carcinomas. Cancer Res 1992;52:3224–7.
[4] Elder JT, Fisher GJ, Lindquist PB, Bennett GL, Pittelkow MR, Coffey Jr RJ, et al. Overexpression of transforming growth factor alpha in psoriatic epidermis. Science 1989;243:811–4.
[5] Stoll SW, Elder JT. Retinoid regulation of heparin-binding EGF-like growth factor gene expression in human keratinocytes and skin. Exp Dermatol 1998;7:391–7.
[6] Shirakata Y, Komurasaki T, Toyoda H, Hanakawa Y, Yamasaki K, Tokumaru S, et al. Epiregulin, a novel member of the epidermal growth factor family, is an autocrine growth factor in normal human keratinocytes. J Biol Chem 2000;275:5748–53.
[7] Nitta H, Kishimoto J, Grogan TM. Application of automated mRNA in situ hybridization for formalin-fixed, paraffin-embedded mouse skin sections: effects of heat and enzyme pretreatment on mRNA signal detection. Appl Immunohistochem Mol Morphol 2003;11: 183–7.
[8] Cook PW, Piepkorn M, Clegg CH, Plowman GD, DeMay JM, Brown JR, et al. Transgenic expression of the human amphiregulin gene induces a psoriasis-like phenotype. J Clin Invest 1997;100:2286–94.
[9] Zhang X, Yang D, Ma S, Liu H. Up-regulation of activities of mitogen-activated protein kinase in psoriatic lesions. J Dermatol Sci 2005;37:118–9.
[10] Sano S, Chan KS, Carbajal S, Clifford J, Peavey M, Kiguchi K, et al. Stat3 links activated keratinocytes and immunocytes required for development of psoriasis in a novel transgenic mouse model. Nat Med 2005;11: 43–9.

Yuji Shirakata*
Department of Dermatology, Ehime University School of Medicine, Shitsukawa, Toon, Ehime 791-0295, Japan

Jiro Kishimoto
Shiseido Research Center, Tsuzuki-ku, Yokohama, Kanagawa, Japan

Sho Tokumaru
Kenshi Yamasaki
Yasushi Hanakawa
Mikiko Tohyama
Koji Sayama
Koji Hashimoto
Department of Dermatology, Ehime University School of Medicine, Shitsukawa, Toon, Ehime 791-0295, Japan

*Corresponding author.
Tel.: +81 89 960 5350;
fax: +81 89 960 5352
E-mail address: shirakat@m.ehime-u.ac.jp
(Y. Shirakata)

19 April 2006

Available online at www.sciencedirect.com
ScienceDirect
Biochemical and Biophysical Research Communications 350 (2006) 315–321
BBRC
www.elsevier.com/locate/ybbrc

Loss of HB-EGF in smooth muscle or endothelial cell lineages causes heart malformation

Daisuke Nanba [a,1], Yumi Kinugasa [a,1], Chie Morimoto [a], Michiko Koizumi [a], Hisako Yamamura [c], Katsuhito Takahashi [c], Nobuyuki Takakura [d], Eisuke Mekada [e], Koji Hashimoto [b], Shigeki Higashiyama [a,f,*]

[a] *Department of Biochemistry and Molecular Genetics, Ehime University Graduate School of Medicine, Shitsukawa, To-on, Ehime 791-0295, Japan*
[b] *Department of Dermatology, Ehime University Graduate School of Medicine, Shitsukawa, To-on, Ehime 791-0295, Japan*
[c] *Department of Medicine, Osaka Medical Center for Cancer and Cardiovascular Diseases, Osaka 537-8511, Japan*
[d] *Department of Signal Transduction, Research Institute for Microbial Diseases, Osaka University, Osaka 565-0871, Japan*
[e] *Department of Cell Biology, Research Institute for Microbial Diseases, Osaka University, Osaka 565-0871, Japan*
[f] *PRESTO, JST, Japan*

Received 22 August 2006
Available online 22 September 2006

Abstract

Epidermal growth factor (EGF) and ErbB family molecules play a role in heart development and function. To investigate the role of EGF family member, heparin-binding EGF-like growth factor (HB-EGF) in heart development, smooth muscle and endothelial cell lineage-specific HB-EGF knockout mice were generated using the Cre/*loxP* system in combination with the *SM22α* or *TIE2* promoter. HB-EGF knockout mice displayed enlarged heart valves, and over half of these mice died during the first postnatal week, while survivors showed cardiac hypertrophy. These results suggest that expression of HB-EGF in smooth muscle and/or endothelial cell lineages is essential for proper heart development and function in mice.

Keywords: Cardiac hypertrophy; Conditional knockout; HB-EGF; Heart valves; Heart failure

Heparin-binding EGF-like growth factor (HB-EGF) is a member of the EGF family of molecules that was first identified in the conditioned media of macrophage-like U-937 cells [1]. HB-EGF is initially synthesized as a type I transmembrane precursor protein (proHB-EGF) that is subsequently enzymatically cleaved to release a soluble form of HB-EGF [1,2]. Further, HB-EGF acts as a mitogen in many different cell types and is involved in a variety of physiological and pathological processes [3–5].

Two independent studies have reported that over half of HB-EGF-null mice die before weaning and that survivors have dysfunctional hearts with grossly enlarged ventricular chambers and reduced life spans [6,7]. Moreover, studies have described the development of enlarged cardiac valves in HB-EGF-deficient mice. This heart valve enlargement has also been observed in EGF receptor (EGFR)-null mice with a CD1 background, in mice with a mutant EGFR (*waved-2*) [8], and in disintegrin and metalloprotease (ADAM) 17-null mice [7], which is a sheddase of proHB-EGF [9,10]. These results indicate that ectodomain shedding of proHB-EGF and subsequent EGFR activation induced by released HB-EGF are crucial for heart valve formation in developmental process as well as development of cardiac hypertrophy in pathological process [11]. However, it is not clear in which of the specific heart cell types (e.g., cardiac myocytes, endothelial cells, and fibroblasts) that HB-EGF expression is required for proper heart development and function.

* Corresponding author. Fax: +81 89 960 5256.
E-mail address: shigeki@m.ehime-u.ac.jp (S. Higashiyama).
[1] These authors contributed equally to this work.

0006-291X/$ - see front matter © 2006 Elsevier Inc. All rights reserved.
doi:10.1016/j.bbrc.2006.09.060

To address this issue, the present study utilized the Cre/*loxP* recombination system for spatiotemporal *HB-EGF* gene ablation. The system generally requires cross-mating of two lines of genetically manipulated mice. One line of mice carries alleles with the *HB-EGF* gene flanked by *loxP* sites [6], and the other line contains a Cre transgene in which the expression of Cre is controlled by *SM22α* or *TIE2* promoter [12,13]. Recombination between the two *loxP* sites in the mated mice results in the catalysis of a deletion of the region flanked by the *loxP* sites (i.e., Cre-dependent transgene expression).

The *SM22α* gene encodes a calponin-related protein that is expressed specifically in adult smooth muscle [14–17]. During mouse embryogenesis, *SM22α* is expressed in cardiac muscle, smooth muscle, and skeletal muscle cells, but becomes restricted to smooth muscle lineages at late embryonic stages and throughout adulthood [18]. The *TIE2* gene encodes an angiopoietin receptor, which is a member of the receptor tyrosine kinase family [19,20]. *TIE2* expression is detected as the first endothelial cells arise, remains positive in endothelial cells throughout development, and is detectable in virtually all endothelial cells of adult tissues [19,21,22].

In this study, we generated smooth muscle and endothelial cell lineage specific HB-EGF knockout mice using Cre/*loxP* system in combination with the *SM22α* and *TIE2* promoter, and demonstrated that HB-EGF in smooth muscle and endothelial lineages was essential for heart development and function.

Materials and methods

Generation of HB-EGF conditional knockout mice using a gene targeting Cre/loxP strategy. Mice with *HB-EGF* gene flanked by *loxP* sites ($HB^{lox/lox}$) were generated as previously described [6]. Homozygous $HB^{lox/lox}$ mice were bred with *SM22α* or *TIE2* promoter-driven Cre-recombinase transgenic mice [12,13] to generate SM22α-Cre:$HB^{lox/WT}$ or TIE2-Cre:$HB^{lox/WT}$ mice. The obtained mice were bred with $HB^{lox/lox}$ mice to generate SM22α-Cre:$HB^{lox/lox}$ (SM22α-Cre:$HB^{-/-}$) or TIE2-Cre:$HB^{lox/lox}$ (TIE2-Cre:$HB^{-/-}$) mice. The genotype of each mouse was confirmed by PCR. Primers are shown in Table 1.

Table 1
Primer sequences for PCR

Wild-type *HB-EGF* (forward)	5′-CATGATGCTCCAGTGAGTAGGCTCTGATTAC-3′
Wild-type *HB-EGF* (reverse)	5′-AGGGCAAGATCATGTGTCCTGCCTCAAGCC-3′
loxP HB-EGF (forward)	5′-ATGGGATCGGCCATTGAACA-3′
loxP HB-EGF (reverse)	5′-GAAGAACTCGTCAAGAAGGC-3′
Cre recombinase (forward)	5′-TTACCGGTCGATGCAACGAGTGATG-3′
Cre recombinase (reverse)	5′-TTCCATGAGTGAACGAACCTGGTCG-3′
SM22α promoter Cre (forward)	5′-CCAGAGAACAGTGAAGTAGGAG-3′
SM22α promoter Cre (reverse)	5′-CATCCAGTCTTGCGAACCTCAT-3′
TIE2 promoter Cre (forward)	5′-CCCTGTGCTCAGACAGAAATGAGA-3′
TIE2 promoter Cre (reverse)	5′-CGCATAACCAGTGAAACAGCATTGC-3′

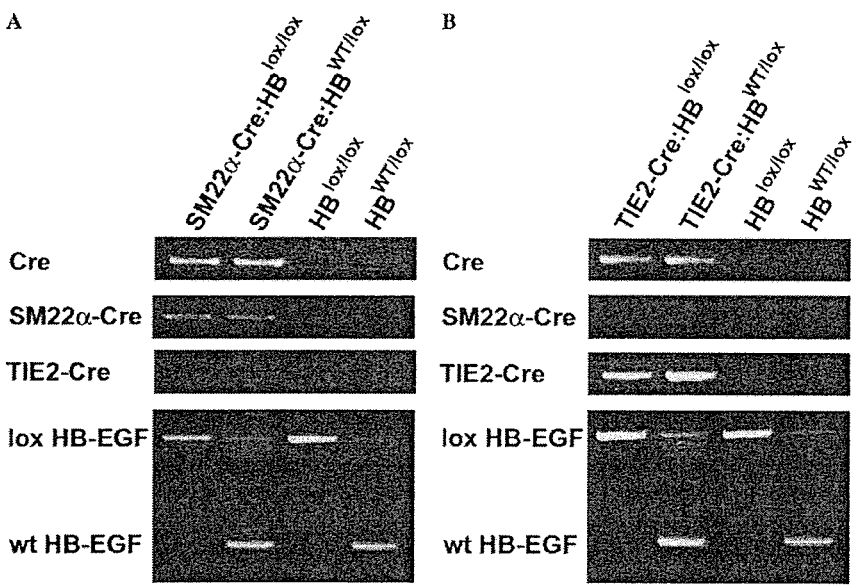

Fig. 1. Genotypes of the conditional knockout mice. SM22α-Cre:$HB^{lox/lox}$ (A) and TIE2-Cre:$HB^{lox/lox}$ (B) mice were confirmed by PCR. *SM22α*-Cre but not *TIE2*-Cre transgenes were detected with SM22α-Cre specific primers and vice versa. The *HB-EGF* gene flanked by *loxP* sites and the wild-type gene were also confirmed by PCR genotyping.